DESIGN OF A CREEP TESTING MACHINE AND STUDY OF GFRP MATERIALS

A Thesis Submitted
In Partial Fulfilment of the Requirements
for the Degree of
MASTER OF TECHNOLOGY

BY
PRAMOD KUMAR SINHA

to the

DEPARTMENT OF MECHANICAL ENGINEERING
INDIAN INSTITUTE OF TECHNOLOGY KANPUR
JULY, 1976

CERTIFICATE

This is to certify that the thesis entitled "Design of a creep testing machine and study of GFRP materials" by P.K. Sinha is a record of the work carried out under my supervision and has not been submitted elsewhere for a degree.

R. Prabhakaran

July 1976

Dr. R. Prabhakaran
Assistant Professor
Dept. of Mech. Engg.
Indian Institute of
Technology, Kanpur

ACKNOWLEDGEMENT

I express my deep sense of indebtedness and gratitude to Dr. R. Prabhakaran for his guidance, encouragement and criticism at all stages of my work.

I am thankful to Dr. V.K. Stokes, Dr. M.M. Oberai, Mr. M. Prasad and other members of faculty and staff of I.I.T., Kanpur for their help at various stages of this work.

I also thank Mr. D.K. Sarkar and Mr. S.L. Srivastava who helped me in various ways.

My thanks are also due to the technical staff of the Central Workshop, I.I.T., Kanpur without whose timely help, fabrication would not have been possible.

I also express my deep sense of appreciation to Dr. D.N. Singh, Prof. S.N. Chakrabarty, my teachers, friends and colleagues of Bihar College of Engineering, Patna who gave me inspiration for higher studies. I can not forget to mention words of acknowledgement to Patna University who sanctioned my deputation to I.I.T., Kanpur for higher studies under Q.I.P.

My thanks are also due to Mr. D.P. Saini for his excellent typing.

And finally I feel very much grateful to my wife Kanti and daughter Sweta who were patient and considerate during the course of this work.

July 1976
I.I.T./Kanpur

P.K. Sinha

CONTENTS

LIST OF TABLES AND FIGURES

Page

Page

$f_L = f_{0^o}$ = Material fringe value for 0^o fibre orientation ($\frac{kg}{cm^2}$ - cm/fringe)

$f_{LT} \approx f_{45^o}$ = Material fringe value for 45^o fibre orientation ($\frac{kg}{cm^2}$ - cm/fringe)

$f_T = f_{90^o}$ = Material fringe value for 90^o fibre orientation ($\frac{kg}{cm^2}$ - cm/fringe)

f_α = Material fringe value for fibre orientation ($\frac{kg}{cm^2}$ - cm/fringe)

α = Fibre orientation angle (degrees)

σ_t = Tangential stress (kg/cm^2)

$(\sigma_t)_{max}$ = Maximum tangential stress (kg/cm^2)

$\sigma_{nominal}$ = Nominal stress (kg/cm^2)

N_α = Fringe order

h = Model thickness (cm)

θ = Angle along the boundary of the notch (degrees)

r = Notch radius (cm)

w' = Width of the specimen across the notch boundary (cm)

P = Applied load (kg)

σ = Applied stress (kg/cm^2)

K_t = Stress concentration factor

E_L = Modulus of elasticity of a composite with fibre orientation angle equal to 0° (kg/cm^2)

E_T = Modulus of elasticity of a composite with fibre orientation angle equal to 90° (kg/cm^2)

G_{LT} = Shear modulus (kg/cm^2)

ν_{LT}, ν_{TL} = Poisson's ratios

e_x = Strain in the direction of load

e_y = Strain in the transverse direction to load

$K_c(t)$ = Creep rupture strength reduction factor

$q_c(t)$ = Notch sensitivity factor in creep

SYNOPSIS

Glass fibre reinforced plastics are being used extensively, as modern engineering materials. Plastics being primarily viscoelastic materials, they creep even at room temperature. Creep data of materials are useful from design point of view when material is intended for long duration use. In the present investigation five similar creep testing machines (loading capacity, 1000 kgs) were designed, fabricated and calibrated as the facility for creep testing was not readily available. Although provision was made in the machine for studying the creep behaviour of GFRP materials at elevated temperature (upto a maximum of about 300°c), actual testing was done only at room temperature. The machines were used for the study of anisotropy of notch sensitivity of a glass reinforced epoxy laminate in creep.

Static and creep tests were conducted for a bidirectionally reinforced composite, for 0° and 45° fibre orientation angles. For static tests, an Instron machine was used. All specimens were tested at a crosshead speed of 0.5 cm per minute. For each fibre orientation three notch

sizes were used. The notch sensitivity was found to be dependent on fibre orientation angle and the biggest notch showed notch-strengthening for 45° orientation.

A particular epoxy resin CY 230 (cured with 12% hardener), which was found to display a notch strengthening effect in low cycle fatigue, was also tested. The polymer exhibited a notch strengthening effect in creep also, especially in the case of the biggest notch.

This study suggests that one of the factors on which the choice of the matrix material is based, can be its notch sensitivity. By properly selecting the matrix, it may be possible to increase - or at least avoid the decrease of - the notched creep rupture strength along fibre orientations where the (unnotched) strength is inherently low.

The results obtained in this investigation also suggest that there may be a relationship between the creep behaviour and the low cycle fatigue behaviour. If such a relationship can be established, then considerable savings in testing time and expenditure can be effected in generating design data.

CHAPTER-I

INTRODUCTION

Glass fibre reinforced plastics are being used extensively as modern engineering materials because of their many desirable properties such as high specific strength (strength/weight), high specific modulus, resistance to corrosion and the ability to provide reinforcement in any required direction. Some of their applications are in aircraft landing gear, helicopter rotor blades, storage containers for chemicals and vehicle bodies.

In metals usually the study of creep has been done at high temperature. But plastics being primarily viscoelastic materials, they creep even at room temperature. Thus it appears logical that study of creep at room temperature should be also done for GFRP materials, if they are to be used for a long duration. The creep behaviour of GFRP materials can be controlled by proper choice of fibres, resins and fibre orientation.

The creep characteristics of most of the metals at high temperature is well understood and at room temperature

they do not show any significant creep. In static loading of ductile metals in presence of stress concentration the increased stress at the root of the notch causes yielding, thereby reducing stress concentration. Because of yielding, the stress becomes nearly uniform inspite of the notch. Under fatigue loading, the stress raisers retain much of their full effect.

The static tensile strength of a notched specimen is often higher than the unnotched tensile strength, because of triaxial stress system at the notch and the smaller volume of material subjected to the maximum stress in the notched specimen. In fatigue, the notch sensitivity at low endurances may become negative.

In the case of GFRP materials it has been generally concluded that under fatigue loading a stress raiser is fully effective in initiating damage but the effect on ultimate failure is small.

Dally and his co-workers (1) pointed out that in the high cycle endurance range the damage at the root of the notch resulted in a changed notch geometry, leading to a reduction in the value of the stress concentration factor, thereby reducing the notch sensitivity. Prabhakaran (2) has recently shown that in low cycle endurance range while

a low notch sensitivity may be exhibited by glass fibre reinforced plastics in general, it is possible for some of them to be almost fully notch sensitive and for others to exhibit even a negative notch sensitivity (notch-strengthening). The information available regarding the creep of composite materials is very limited. Detailed investigations regarding the effect of stress concentration, etc. on the creep rupture strength are almost non-existent.

An experimental study of the anisotropy of notch sensitivity in creep of a commercially obtained glass fibre reinforced epoxy was undertaken in the present work.

As facility for creep testing was not readily available, a creep testing machine was first designed, fabricated and calibrated. Creep is a long duration test and scatter is a common phenomenon in GFRP materials, and so five similar testing setups were fabricated, so that large number of specimens could be tested simultaneously. The maximum loading capacity of the creep testing setup was approximately 1000 kgs. The main design features of the creep testing machine are described in chapter II.

The effect of the fibre orientation angle, although a very important parameter, could not be studied thoroughly due to shortage of commercial composite sheets. However,

0° and 45° fibre orientations were studied. A study of notch sensitivity under static loading for both fibre orientation angles of commercial composite was also done.

A previous study of the notch sensitivity of polymers (3) had shown that the epoxy resin CY 230 cured with 12% hardener exhibited similar behaviour compared to the 45° composite. In this investigation the influence of stress concentrations on the room temperature creep strength of the same epoxy material CY 230 (cured with 12% hardener) was studied.

The creep notch sensitivity behaviour of the 45° composite was found to be very similar to that of the CY 230 epoxy. This suggests that the notch strengthening effect in a composite is due to the matrix.

The results of this investigation are important in two respects. First, they confirm previous findings of Prabhakaran and Nair that a composite can exhibit a notch strengthening effect which can be attributed to the matrix. Secondly, the similarity in the previous low cycle fatigue test results and the present creep results indicates that it should be possible to establish some kind of a relation between the two types of tests. As both fatigue and creep tests are time consuming and expensive, the possibility of avoiding one type of tests holds great promise to the material engineer.

CHAPTER-II

DESCRIPTION OF CREEP TESTING MACHINE

2.1 Introduction

A material subjected to constant stress and exhibiting time dependent strain is said to creep. When a specimen which creeps is subjected to a constant tensile load, the change in average stress due to Poisson's effect is usually quite small and hence it is an established experimental practice to conduct creep test at constant load in place of that at constant stress. Creep test is usually conducted at constant temperature as with the change of temperature, the rate of creep also changes. In view of creep being a long duration test accompanied by appreciable scatter in the case of composite materials, five similar creep testing machines have been fabricated to enable simultaneous testing of large number of specimens.

The main design features of the creep testing machine (Figure 2.1) are as follows:

(a) loading by dead weight,

(b) amplification of dead weight load by a double lever system,

(c) vertical movement of specimen under creep deformation by Peaucellier cell mechanism,

(d) prevention of twisting of specimen at the time of fixing by specimen holder at lower end,

(e) maintaining constant temperature in furnace by temperature controller,

(f) specimen fixture in grips without slip,

(g) measurement of overall extension of specimen by LVDT,

(h) measurement of time to fracture, by automatic stoppage of a clock mechanism at the time of specimen fracture.

Calibration of creep testing machine has been done with respect to Instron machine and corrections have been made in LVDT sensed transducer-amplifier-recorder extension readings for the elastic deformation of machine linkages under various loads. The main design features of the machine and the calibration and correction procedures are described in the following sections.

2.2 Description of Creep Testing Machine

Constant load on a specimen can be applied by putting dead weights on pans attached to either ends of the long lever, 1 (Figure 2.2). The long lever is pivoted at point A on the left pillar, 15. The bigger arm of the long lever gives higher lever ratio when dead weights are placed on the

right end of the long lever whereas the smaller arm gives a smaller lever ratio when dead weights are placed on the left end of the long lever. The transfer of load from the long lever to the specimen takes place through a double lever system and a Peaucellier cell mechanism. The use of a double lever system, consisting of long lever,1, and short lever,2, makes the machine compact and increases the lever ratio. The dead weights have been made in such combinations that in the range of 0 to 26 kgs any weight can be put on the pan in steps of 100 gms. When the long lever is moved up or down the Paucellier cell mechanism (Figure 2.3) receives circular motion at point B from the short lever and delivers straight line motion at point C to the connecting link,6, thus preventing sideway shift of specimen upper end. A pair of Peaucellier cell mechanisms, one on either side of the lever, distributes the load symmetrically and makes the line of action of the load on the specimen coincide with the centre line of the specimen. Two pillars, 15 support the levers, furnace and a bridge,16. The bottom specimen holder,9, passes through a hole in the bridge. The threaded portion of the bottom specimen holder has a keyway slot along its length. A key passing through the bridge engages the bottom specimen holder and when the nut is tightened over the threaded portion of bottom specimen holder, the key prevents its rotation, but allows up or down movement in a straight line. Thus the

key prevents the twisting of the specimen at the time of fixing in the machine. The grip (Figure 2.4) has a one mm. deep recess with a width equal to the specimen width, in which the specimen fits. The surface of the grip in the recess has been made rough by making serrations to avoid slipping of specimens in the grip during the test. The furnace for maintaining constant temperature of specimen consists of an aluminium furnace tube over which a heating tape is wound. The annular space between the furnace tube and the furnace casing is filled with insulating material to prevent leakage of heat to atmosphere. The temperature in the furnace is sensed by a thermocouple and its output is used as control signal to actuate the temperature controller.

The creep extension is measured by means of an LVDT transducer. The LVDT is connected at point C and its output is recorded by a transducer-amplifier-recorder. As the extension in the specimen increases with time, the long lever goes down and the LVDT sensing tip is released so that when the specimen fractures, the moving parts of the machine do not strike the LVDT. A counter coupled to a constant speed electric motor has been used as the time indicator. When the fracture of a specimen takes place, the smaller arm of the long lever moves up, which in turn pulls up the knob

of an electric switch. Thus the electric motor stops and the counter indicates the time at fracture. With one of the machines , an electric clock has been used directly.

2.3 Calibration

The creep testing machine has been designed to apply a maximum axial load of 1000 kg. A mild steel strip (22.9 cm long, 3.7 cm wide and 0.32 cm thick) was used as the calibration specimen to determine the lever ratio and the equivalent load due to the weight of the lever system. Four SA-12 strain gauges were mounted on the calibration specimen, two on each side, to measure the axial and transverse strains. The gauges were connected on the appropriate arms of a Wheatstone bridge, so that there was a signal addition and increased sensitivity.

The calibration specimen was loaded in tension on the Instron machine and the strain gauge readings were noted at several load levels. Next the calibration specimen was loaded in a creep testing machine and again the strain gauge readings were noted at different load levels. A typical calibration curve is shown in Figure 2.5. The ratio of the slope of the load-strain curve obtained on the Instron machine to the slope obtained on the creep testing machine gives the lever ratio for the particular creep setup. Other details calculated from the graph are listed

in table 2.1.

TABLE 2.1

Details of Calibration of Creep Testing Machine No.3

Lever ratio with loading pan connected to bigger arm of long lever	35.4
Lever ratio with loading pan connected to smaller arm of the long lever	8.73
Effective load on specimen due to unbalanced dead weight and loading pan connected to bigger arm of long lever	173 kgs
Effective load on specimen due to unbalanced dead weight and loading pan connected to smaller arm of the long lever	76 kgs
Effective load on specimen due to unbalanced dead weight and loading pan connected to both ends of the long lever	148 kgs

The calibration procedure described above was repeated for all the creep testing machines.

One SA-12 strain gauge was mounted on connecting link, 6, of machine number 2, to measure the longitudinal

strain. With the mild steel calibration specimen fixed on machine number 2, a 24 hour test at a relatively high load (the maximum load used in later tests) showed almost no variation in the strain reading, which ensured that there was no creep in the machine linkages. In a separate test on the calibration specimen, the axial strain indicated by the longitudinal gauges was noted while loading in the Instron. Then the calibration specimen was loaded in the creep testing machine and the total elastic deformation in the linkages and the specimen was noted as a function of the applied load, by means of the LVDT. A creep deformation correction chart was prepared by subtracting the elastic deformation in the calibration specimen (given by the Instron test) from the total elastic deformation in the linkages and the calibration specimen (given by the LVDT readings). A typical correction curve is given in Figure 2.6.

While the extension of the creep specimen proceeds, the long lever of the machine moves down. The lever has been held in various positions by adjusting the nut attached to the bottom specimen holder. The strain readings indicated by strain indicator for the calibration specimen showed little variation, thus ensuring that the load on the specimen remained constant even though the position of the long lever changed.

The LVDT output has been recorded by a transducer-amplifier-recorder. The recorder full range has been calibrated for full range displacement of LVDT tip with the calibration kit. The displacement given to LVDT has been measured with the micrometer supplied with it. A typical calibration graph between LVDT tip displacement and recorder readings is shown in Figure 4.7 and a typical value of calibration scale for machine number 3 is listed in table 2.2.

The time recorder was run for 24 hours and the calibration scale for the counter reading has been calculated and a typical value for machine number 3 is listed in table 2.2.

TABLE 2.2

Calibration Scale for LVDT and Time Recorder Connected to Creep Testing Machine Number 3.

One small division of LVDT sensed transducer-amplifier-recorder reading	7.89×10^{-3} cm
One division of time recorder	0.2 minute

2.4 Loading Procedure

Before a specimen was loaded, the unbalanced weight of the machine parts was neutralized by placing proper dead

weights on the smaller arm of the long lever. The specimen was then placed in the proper position and by tightening the nut attached to the bottom specimen holder the lever was adjusted so that the transducer-amplifier-recorder showed a sufficiently large reading. Holding the lever in the same position, proper dead weights were placed on the pan and then the lever was allowed to fall slowly so as to avoid shock loading. Simultaneously the timer was also switched on.

The creep testing machine after installation and calibration has been found to be quite satisfactory. The machines have been used for studying the room temperature creep of GFRP materials and succeeding Chapters describe the tests.

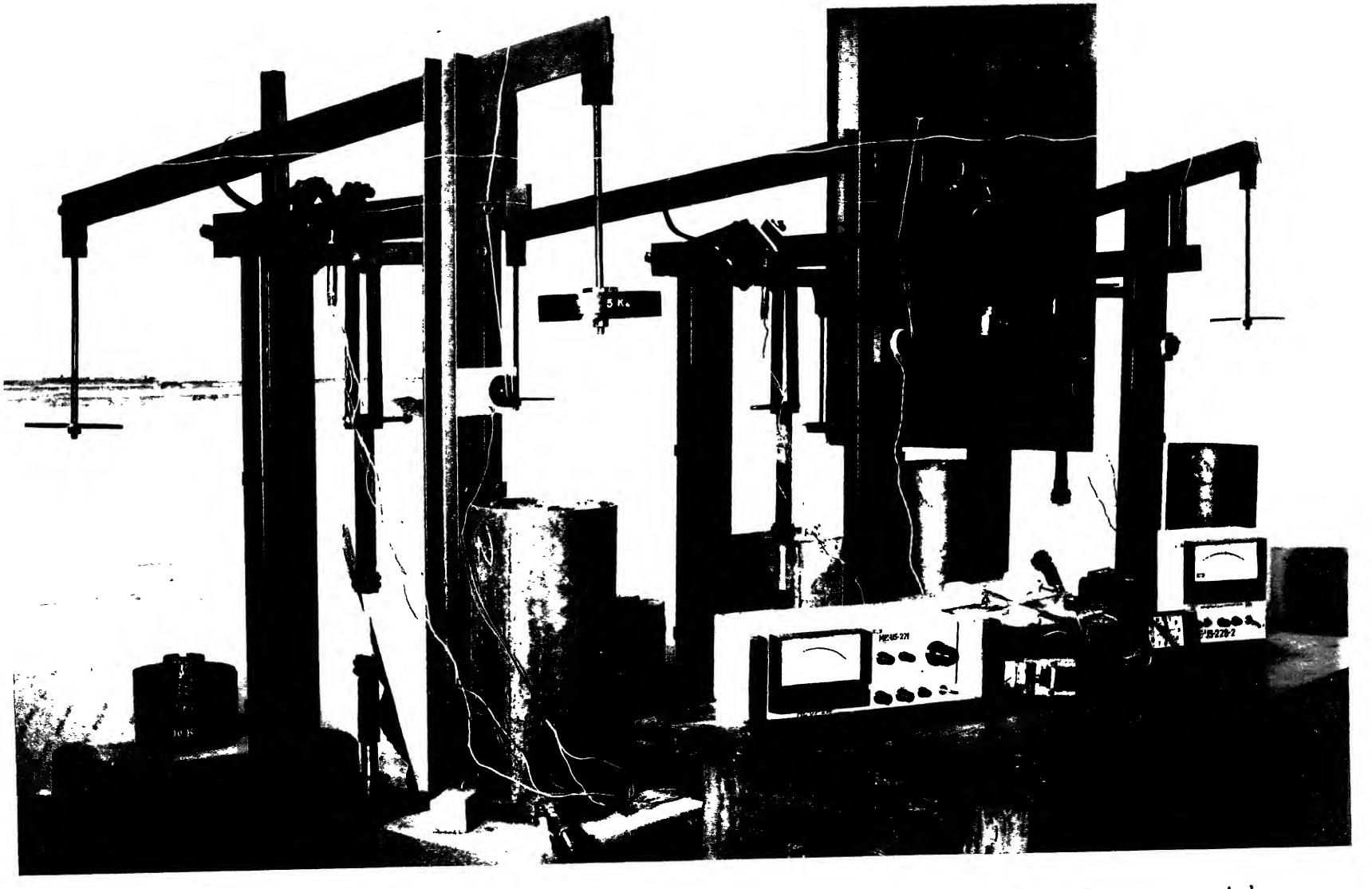

Fig.2.1 Photograph showing main features of creep testing machine

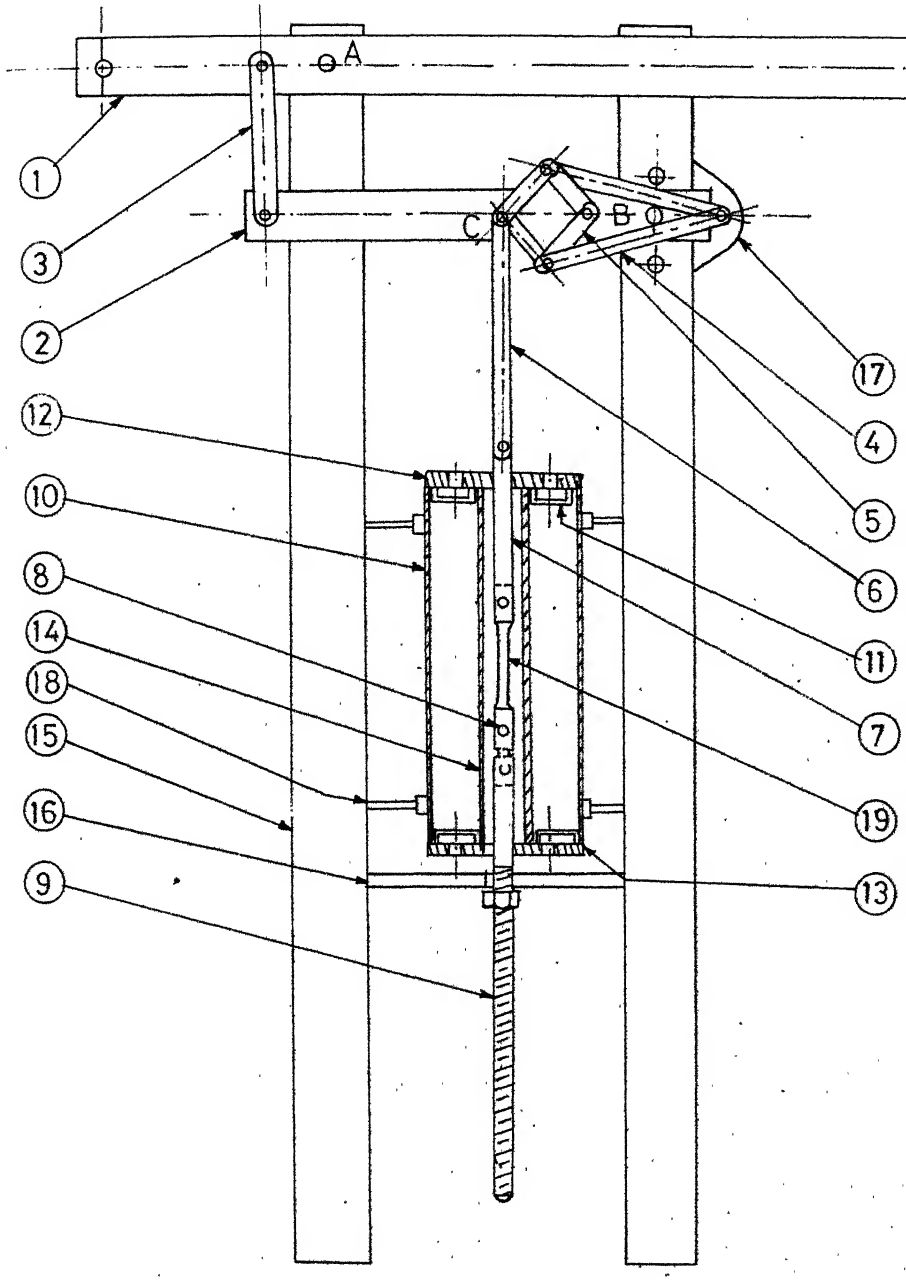

Sl. No.	Parts Name
1.	Long leaver
2	Short leaver
3	Lever connecting link
4	P.C. Connecting
5	Rhombus link
6	Connecting link
7	Top specimen holder
8	Bottom specimen holder link
9	Bottom specimen holder
10	Furnace casing
11	Furnace casing cover
12	Top insulated cover
13	Bottom insulated cover
14	Furnace tube
15	Pillar
16	Bridge
17	Bracket
18	Furnace holder
19	Specimen

2·2 SCHEMATIC SKETCH SHOWING DETAILS OF CREEP TEST MACHINE.

Fig. 2.3 Photograph showing the Peaucellier cell mechanism and specimen

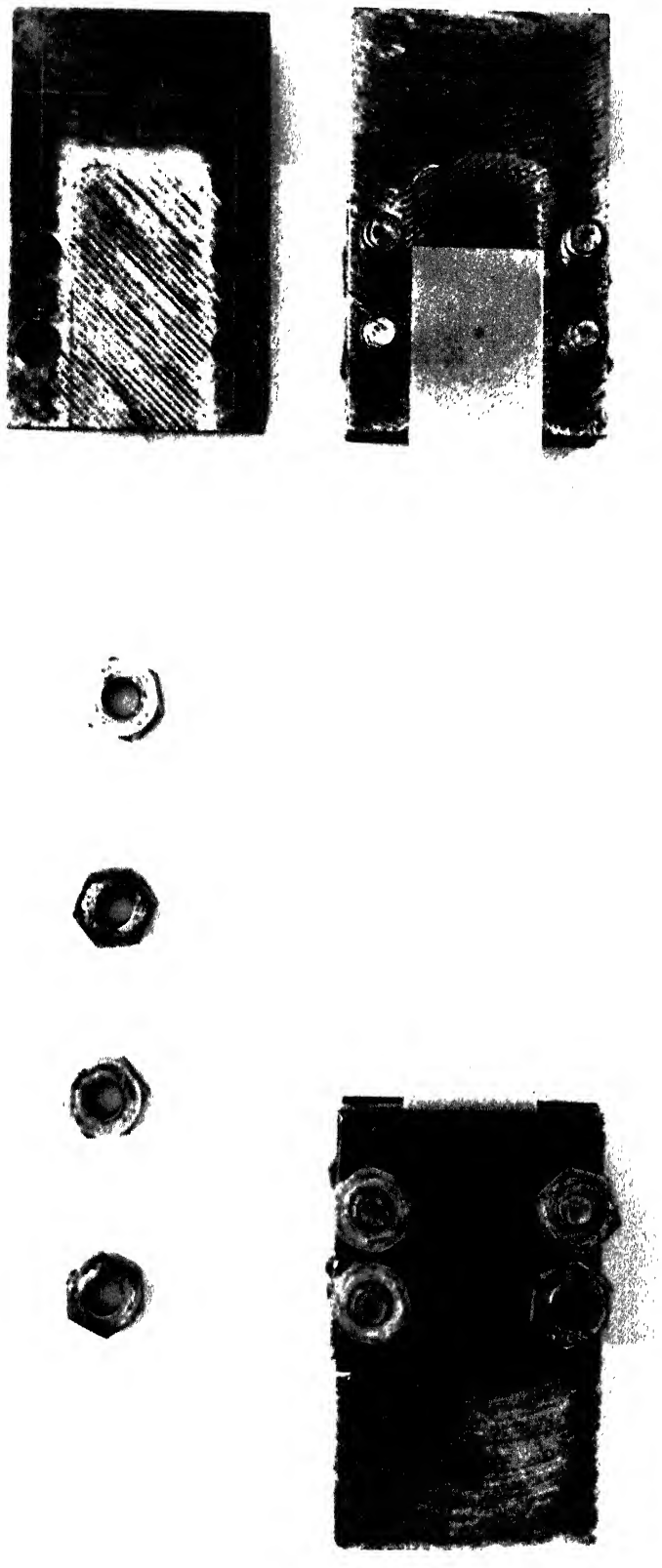

Fig.2.4 Photograph showing details of grip

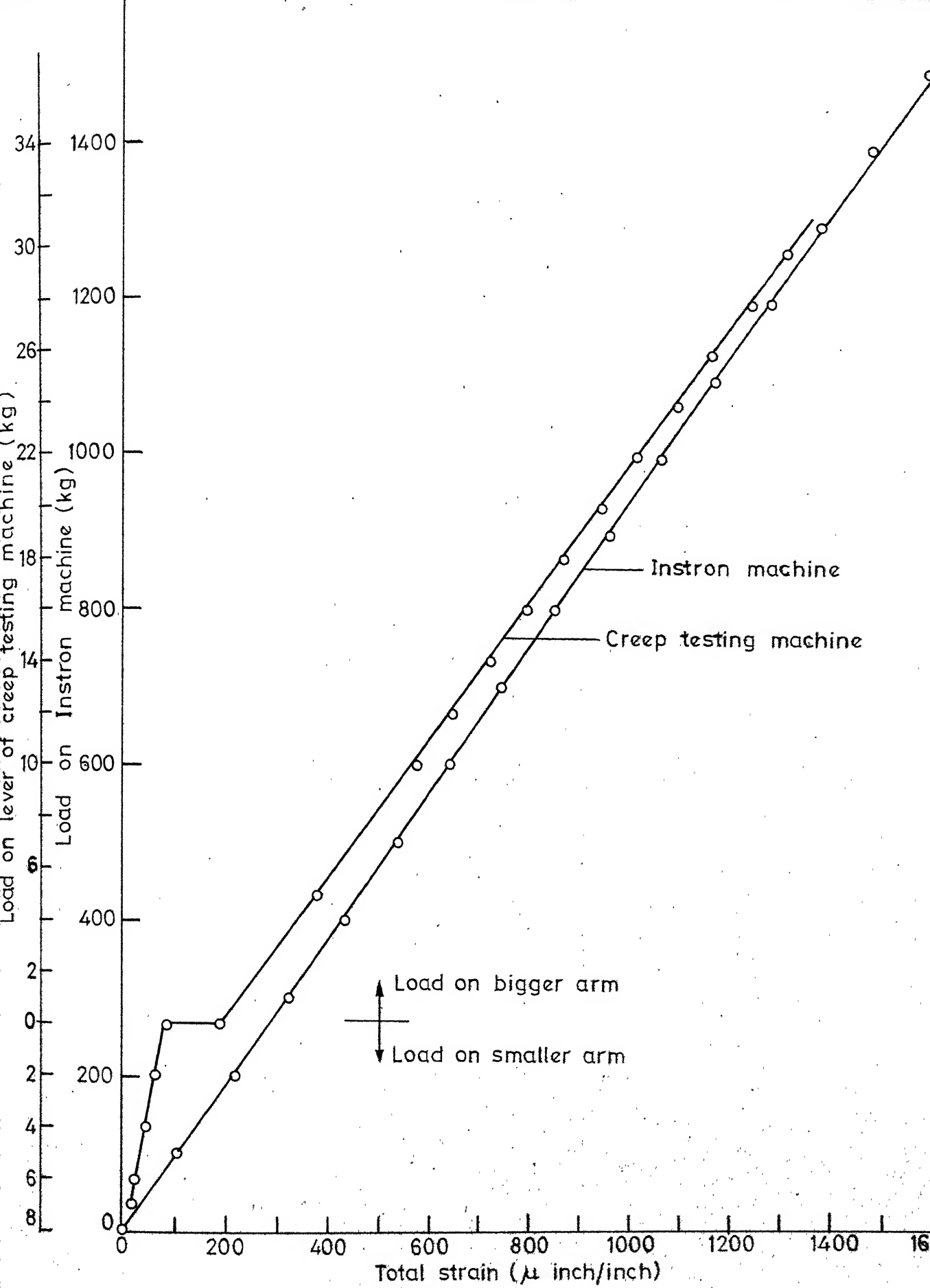

Fig.2.5 Calibration curve for creep testing machine-3

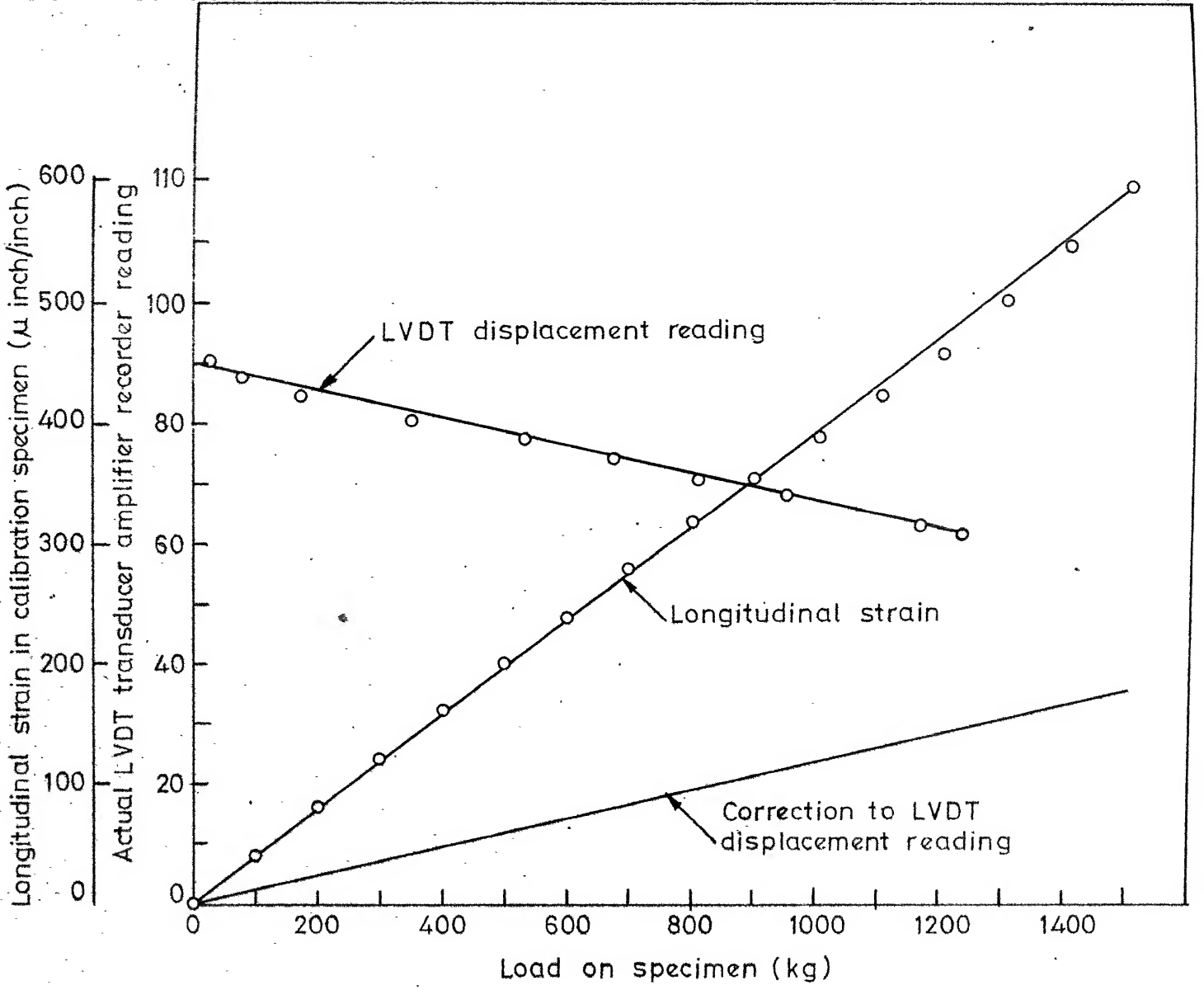

Fig.2.6 Correction curve for LVDT signal on machine

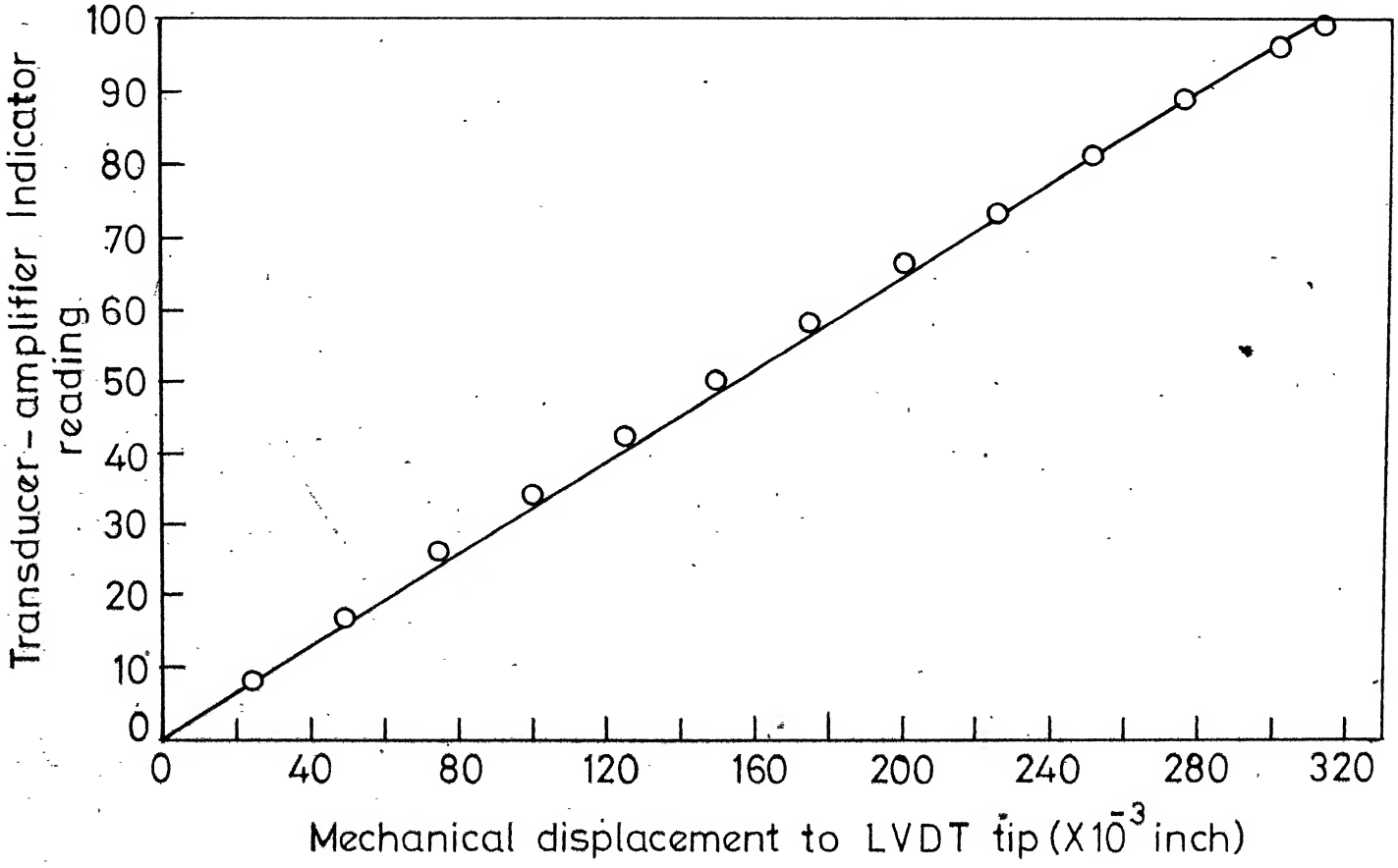

Fig. 2.7 Calibration curve for LVDT

CHAPTER-III

DETERMINATION OF STRESS CONCENTRATION FACTORS

Stress concentration factors for various notch geometries in anisotropic materials are not as readily available in the literature as in the case of isotropic materials. Theoretical solutions are scarce and are confined to notches in infinite plates (4). While numerical solutions and experimental methods are more suited for anisotropic materials, such results are also not readily available. In this chapter, the transmission photoelastic technique of determining stress concentration factors in composite materials is briefly described.

As the notch sensitivity was experimentally determined for bidirectionally reinforced (balanced equal reinforcements in both directions) composites in the 0° and 45° orientations, the elastic stress concentration factors were determined for these orientations by employing the methods of photo-orthotropic elasticity developed recently (5,6,7).

The model material utilised was an E-glass-fibre-reinforced polyester, with the matrix, specially blended to

produce a refractive index almost exactly equal to that of the reinforcement. Photoelastic calibration specimens (for tensile loading) for 0^{o}, 45^{o} and 90^{o} were machined and material fringe values were determined in a transmission polariscope using sodium light. They are

$$f_L = f_{0^o} = 207 \ \frac{kg}{cm^2} \text{ - cm/fringe}$$

$$f_{LT} \approx f_{45^o} = 75 \ \frac{kg}{cm^2} \text{ - cm/fringe}$$

$$f_T = f_{90^o} = 195 \ \frac{kg}{cm^2} \text{ - cm/fringe}$$

The material fringe values for any fibre orientation angle (for uniaxial stresses) can be calculated using the equation

$$\left(\frac{1}{f_\alpha}\right)^2 = \left(\frac{\cos^2\alpha}{f_L} - \frac{\sin^2\alpha}{f_T}\right)^2 + \frac{\sin^2 2\alpha}{f_{LT}^2} \qquad (3.1)$$

where α is the fibre orientation angle with the stress direction. The usual approximation (good to about 2% or better) that f_{LT} and f_{45^o} are equal, is made.

Semi-circular side notched specimens were machined from the photoelastic model material with notch parameters $2r/w = 0.130$, 0.375 and 0.740. The specimen geometries are given in Figure 3.1. Each specimen was loaded in tension

and the resulting dark-field and light-field isochromatic fringe patterns were photographed. There was no residual isochromatic response because of the balanced construction. The maximum fringe order on the notch boundary gives directly the maximum tangential stress, σ_t, in isotropic materials. In the case of anisotropic materials, the variation of material fringe value along the notch boundary also has to be considered. The maximum tangential stress is given by

$$(\sigma_t)_{max} = \frac{(N_\alpha \cdot f_\alpha)_{max}}{h} \qquad (3.2)$$

where h is the model thickness. The fringe order, N_α, the material fringe value, f_α, and the stress ratio $(N_\alpha f_\alpha w'/P)$ are shown as a function of θ, along the boundary of the notch for 45° fibre orientation and notch parameter $2r/w = 0.740$ in Figure 3.2, where θ, r, w' and P are respectively the angle along the notch boundary, notch radius, width of the specimen across the notch boundary and the applied load. The stress ratio $\sigma_t/\sigma_{nominal}$ varies along the boundary of the notch and need not be, in general, maximum where σ_t is maximum. The maximum value of the stress ratio was taken as the stress concentration factor and it is given by

$$K_t = \frac{(N_\alpha \cdot f_\alpha \cdot w')_{max}}{P} \qquad (3.3)$$

The stress concentration factors determined by the above method are given in the following table. Stress concentration factors for isotropic materials, given by R.E. Peterson (8) are also listed in the table 3.1.

TABLE 3.1

Stress Concentration Factors

Fibre Orientation Angle (degrees)	Notch Parameter		
	2r/w = 0.130	2r/w = 0.375	2r/w = 0.740
0°	2.80	2.15	1.66
45°	1.94	1.65	1.42
Isotropic Material	2.68	1.93	1.2

The above values were used along with the creep strength reduction factors, in computing the notch sensitivity factors. These factors are defined in the next chapter and the creep results for a composite and a polymer are also described.

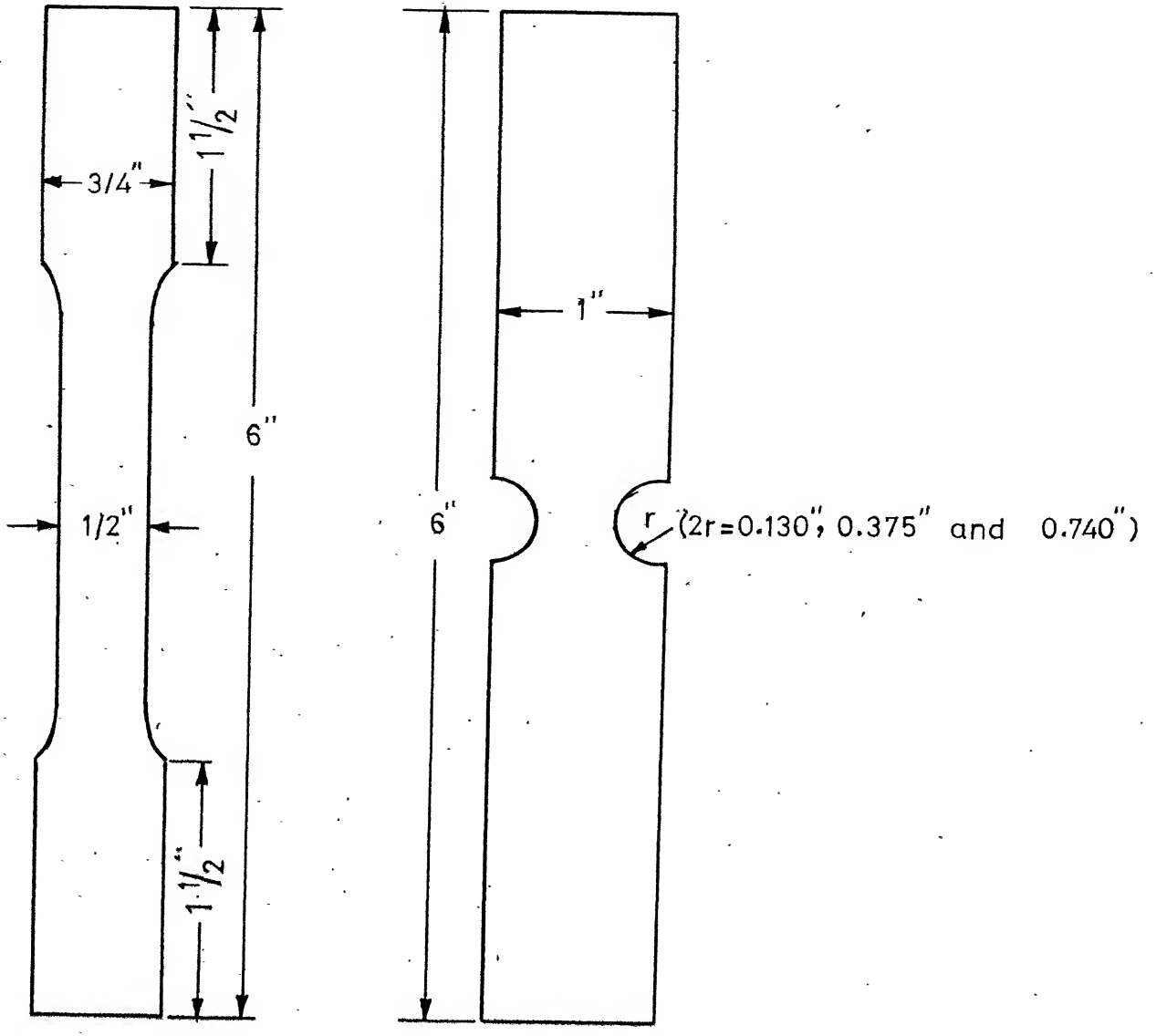

Fig.3.1 Specimen Geometries

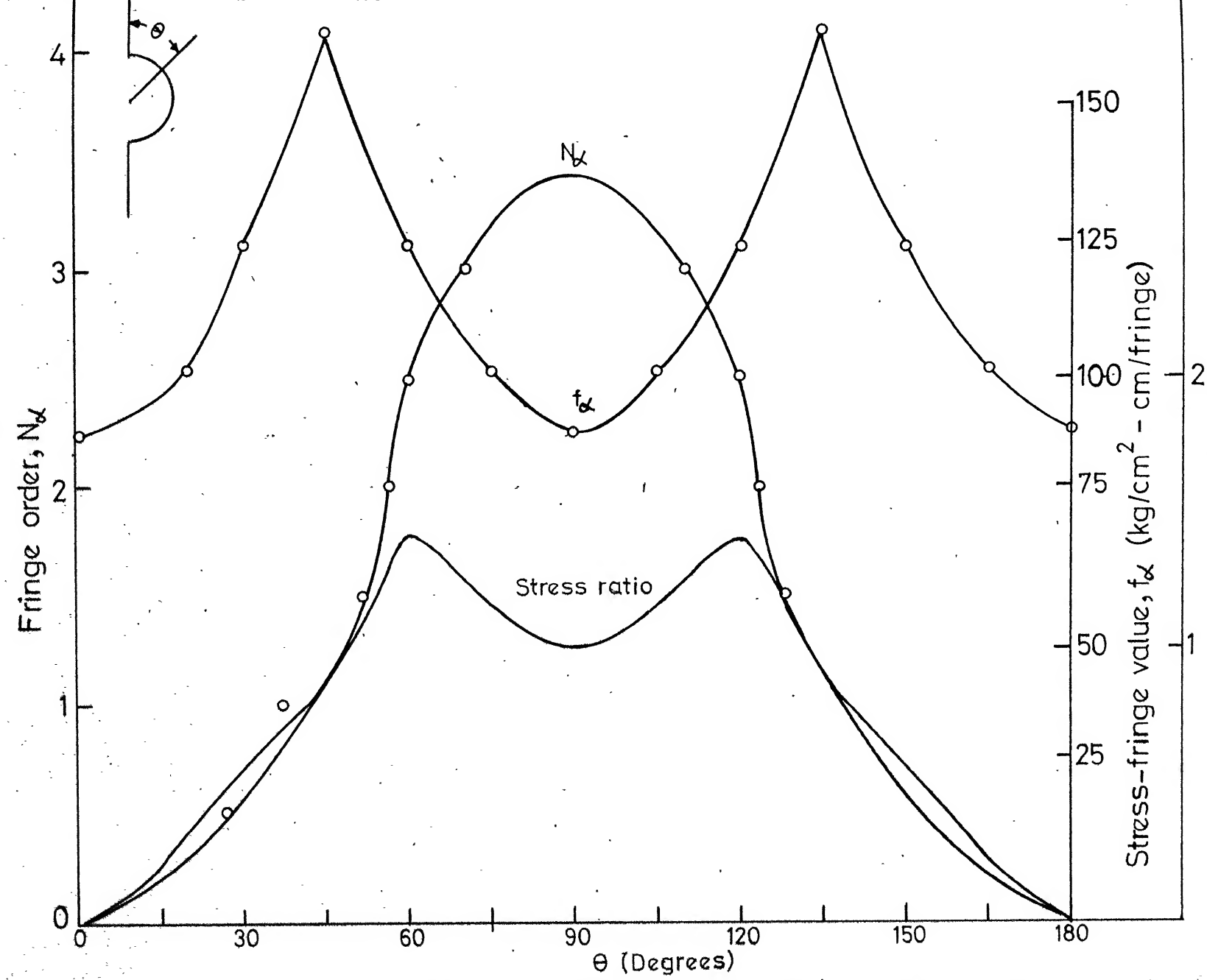

Fig 3.2 Variation of fringe order (N_α) material fringe value (f_α) and stress ratio along the

CHAPTER-IV

EFFECT OF STRESS CONCENTRATIONS ON THE ROOM TEMPERATURE CREEP RUPTURE STRENGTH

4.1 Introduction

In many applications composite structures are subjected to constant sustained loads at room temperature or at elevated temperatures. The presence of intentional (that is, functional) or unintentional stress concentration in the form of sudden changes in geometry is also quite common. For the design of such structures, it is necessary to know the behaviour of composite materials under the combined effect of creep and stress concentrations.

The two constituents of a glass fibre reinforced plastic are known to have time-dependent strength. In the case of the glass reinforcement the phenomenon is known as 'static fatigue' and is mainly due to the effect of moisture in the ambient atmosphere on the glass. In the case of matrix the phenomenon (of time-dependent strength) is due to the viscoelastic nature of the polymer. In a composite the glass fibres are effectively protected by the matrix from ambient

humidity but the viscoelastic behaviour is also imparted by the matrix (9).

The anisotropy of composite properties is well recognized in respect of static strength, elastic constants and fatigue strength. The information available in technical literature on the anisotropy of creep properties of composites is very limited (10-13) and practically no information is available regarding the effect of stress concentrations on the creep strength (14).

This chapter describes the room temperature creep strength of a commercial composite. The fibre orientation angle and the notch parameter were used as experimental variables. As the matrix which was used in the composite could not be procured from the supplier, an epoxy resin whose low cycle fatigue properties were known, was tested in creep. The results for the epoxy are also given in this chapter.

4.2 Characterization of the Composite Material

The glass fibre reinforced plastic material studied in this investigation was a bidirectionally reinforced commercial laminate (60 cms X 60 cms X 0.32 cm) made of E-glass fabric and epoxy matrix. The laminates had almost equal amounts of reinforcement in two perpendicular directions.

The fibre volume fraction, determined by resin burnout test, was 36.5 percent.

Five intrinsic macroscopic inplane material properties E_L , E_T , ν_{LT} , ν_{TL} and G_{LT} are required for characterisation of an orthotropic material. The method suggested by Greszczuk (15) was used to measure these five elastic constants. Three tensile specimens were machined, one each for fibre orientations of 0^o, 45^o and 90^o. Two strain-gauges, one axial and another transverse were fixed on each test specimen and tested in an Instron machine. Once the stress-strain relationship is established, the determination of elastic constants is straight forward. The shear modulus G_{LT} was obtained from the relation

$$G_{LT} = \frac{\sigma}{2(e_x - e_y)} \qquad (4.1)$$

where e_x and e_y are the strains recorded in the loading and transverse directions of 45^o specimen and σ is the applied stress. The measured elastic constants are given below

$E_L = 0.222 \times 10^6$ kg/cm^2

$E_T = 0.196 \times 10^6$ kg/cm^2

$\nu_{LT} = 0.203$

$\nu_{TL} = 0.181$

$G_{LT} = 0.042$ kg/cm^2

The static tensile strengths of unnotched specimens were measured on the Instron machine at 0.5 cm/minute crosshead speed for both 0° and 45° fibre orientation angle. The results of static tests are given in table 4.1.

TABLE 4.1

Static Tensile Strengths of Unnotched Specimens

Fibre Orientation Angle	Specimen Number	Static Tensile Strength(kg/cm^2)	Mean Static Tensile Strength(kg/cm^2)
0°	1	1560	
0°	2	1535	1535
0°	3	1516	
0°	4	1545	
0°	5	1521	
45°	1	1152	
45°	2	1162	
45°	3	1198	1164
45°	4	1160	
45°	5	1150	

4.3 Effect of Notches on the Creep Rupture Strength of the Composite

The dimensions of the unnotched and notched composite specimens for the creep tests were the same as those for the determination of stress concentration factors, shown in

Figure 4.1. Due to the limited supply of material, only the 0° and 45° orientations were tested. For each orientation, all the three notch sizes were studied.

Each set of specimens (particular orientation, particular notch parameter value) was subjected to various fractions of its static tensile strength and the extension was noted as a function of time. When complete fracture occurred, the time was noted.

Typical results for the creep rupture strength, illustrating scatter in the values, are shown in Figure 4.1. Approximately fifteen specimens were tested for each set of experimental variables and the best fitting straight lines were drawn. Consolidated results for 0° orientation and 45° orientation are given in Figure 4.2 and 4.3, respectively. In the case of 0° orientation, all the three notches are seen to reduce the room temperature creep rupture strength. The effect of the biggest notch is very small but surprisingly, it is the intermediate notch - and not the smallest - that reduces the strength the most. In the case of 45° orientation, the biggest notch increases the creep rupture strength above the unnotched strength. This is evident from Figure 4.3 which also shows that the other two notches reduce the strength, though only slightly. The notch-strengthening

effect in the case of the 45° orientation is discussed in detail later in this chapter.

Creep curves for the unnotched specimens of the 0° and 45° orientations are shown in Figure 4.4 and 4.5 respectively. As is to be expected, the creep extension is significantly greater for the 45° orientation and besides, the creep extension increases steeply just before fracture. This would correspond to the third stage of creep in a standard creep curve and is absent in the case of the 0° orientation.

In evaluating the effect of notches on the creep rupture strength, the same procedure as in the case of fatigue is adopted. First the creep rupture strength reduction factor, K_c is defined as

$$K_c(t) = \frac{\text{creep rupture strength of unnotched specimen}}{\text{creep rupture strength of notched specimen}} \quad \ldots \quad (4.1)$$

It is evident that the creep rupture strength reduction factor is a function of time. The notch sensitivity factor in creep, q_c , is then defined as

$$q_c(t) = \frac{K_c(t) - 1}{K_t - 1} \quad (4.2)$$

where K_t is the theoretical stress concentration factor.

The creep notch sensitivity factor was determined for 0° and 45° orientations from Figures 4.2 and 4.3 and is shown in Figures 4.6 and 4.7. In the case of the 0° orientation the notch sensitivity factor is almost independent of time for all the three notch sizes. For the 45° orientation, there is a general tendency for the notch sensitivity factor to increase with time. It is also interesting to note from Figure 4.7 that q_c is negative in the case of the biggest notch; this is a consequence of Equation (4.2) and the previously mentioned notch strengthening effect.

4.4 Effect of Notches on the Creep Rupture Strength of a polymer

The unusual phenomenon of notch-strengthening of glass fibre reinforced plastics, especially for the 45° orientation and the largest notch has been observed in the case of creep rupture strength (Section 4.4) and also in the case of low cycle fatigue strength (2). As the matrix plays a dominant role in the case of 45° orientation, this notch strengthening effect can be expected to be due to the matrix alone. For the commercial composite it was known that the matrix used was an epoxy resin but attempts to procure sheets of this matrix from the supplier were not successful.

In order to obtain some idea of the notch sensitivity of polymers in creep, an epoxy resin, CY 230, cured

with 12% hardener was studied in creep loading. This resin was selected as it has been found to exhibit negative notch sensitivity in low cycle fatigue (3). The specimen geometries and the creep testing procedure were identical as in the case of composite specimens.

The variation of the creep rupture strength with time is shown in Figure 4.8 for unnotched and notched specimens. Again the biggest notch is seen to raise the creep rupture strength above that of the unnotched material. The intermediate and smallest notches reduce the strength.

Creep curves for the epoxy resin unnotched are shown in Figure 4.9. For all the stress levels shown, there is a steep increase of the extension from the beginning, indicating that the third stage of creep is dominant. It should again be emphasized here that the load was maintained constant on the specimens and the constancy of stress is based on the assumption that the area of cross section does not change appreciably.

From the creep rupture strength verses time curves shown in Figure 4.8 and from Equation (4.2), the creep notch sensitivity factor, q_c , was determined. The dependence of q_c on time is shown in Figure 4.10 for the three notches.

The smallest and the intermediate notches give rise to positive, but small, notch sensitivity, with the intermediate notch becoming more detrimental (in terms of q_c) beyond about 200 minutes. The notch sensitivity factor for the biggest notch is negative and the notch strengthening effect increases with time.

4.5 Comparison of Creep Notch Sensitivity of Composite (0° and 45° orientations) and Polymer

Apart from establishing the notch sensitivity of a composite as a function of the fibre orientation angle, another aim of the investigation was to relate the matrix behaviour to the composite behaviour in terms of notch sensitivity. The thermosetting polymer CY 230 (cured with 12% hardener) was considered, based on its low cycle fatigue properties, to represent qualitatively, the behaviour of the actual polymeric matrix used in the commercial composite.

The notch sensitivity factors for the composite (0° and 45° orientations) and for the epoxy resin are shown as a function of the notched parameter under static loading in Figure 4.11. As mentioned earlier, the 0° composite exhibits positive, but relatively low notch sensitivity for all the notch sizes. The behaviour of the 45° composite and the epoxy is very similar in that the notch sensitivity is

positive but very small for the smallest notch and it becomes negative for the biggest notch.

The measured creep notch sensitivity factor is shown as a function of the notch parameter for all the three materials for 10 minutes and 10,000 minutes in Figures 4.12 and 4.13, respectively. It is seen that these results are very similar to those of Figure 4.11.

4.6 Additional Creep Results

In a typical creep experiment, the variation of the creep rupture strength as a function of time is only part of the experimental data. From the record of creep deformation as a function of time, it should be possible to determine the dependence of the strain-rate on the stress level and it should also be possible to construct the isochronous stress-strain curves.

In the present investigation, tests were terminated after a relatively short time, in otherwords, the stress levels employed were relatively high compared to the static strength. It may be said that the present tests bear the same relation to creep tests in general as low cycle fatigue testing bears in relation to fatigue tests in general. Because of the absence of long - time creep data, the information

available regarding creep rate and the isochronous stress-strain behaviour is very limited.

Isochronous stress-strain curves for the CY 230 epoxy cured with 12% hardener are shown in Figure 4.14. For comparison the tensile stress-strain curve for monotonic loading is also shown.

The maximum extension at creep fracture is shown as a function of the creep stress level for the epoxy in Figure 4.15. The figure indicates that as the stress level is decreased, leading to longer life, the creep extension at fracture increases. Limited results on the same lines for the 45° composite are shown in Figure 4.16. This figure also shows the same trend of increasing creep extension for decreasing stress level and increasing time under load.

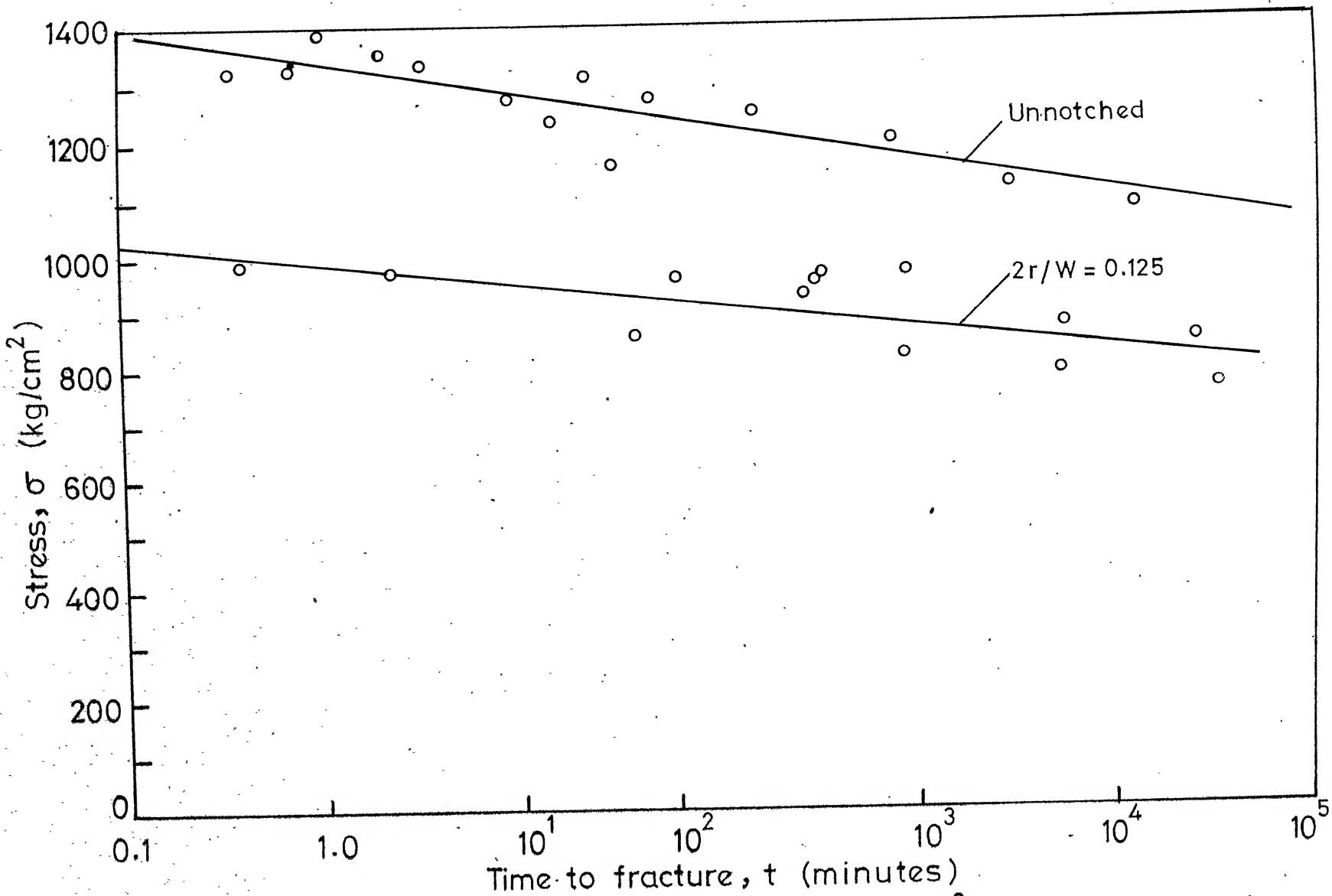

Fig. 4.1 Typical stress vs. time to fracture results for 0° composite, showing scatter

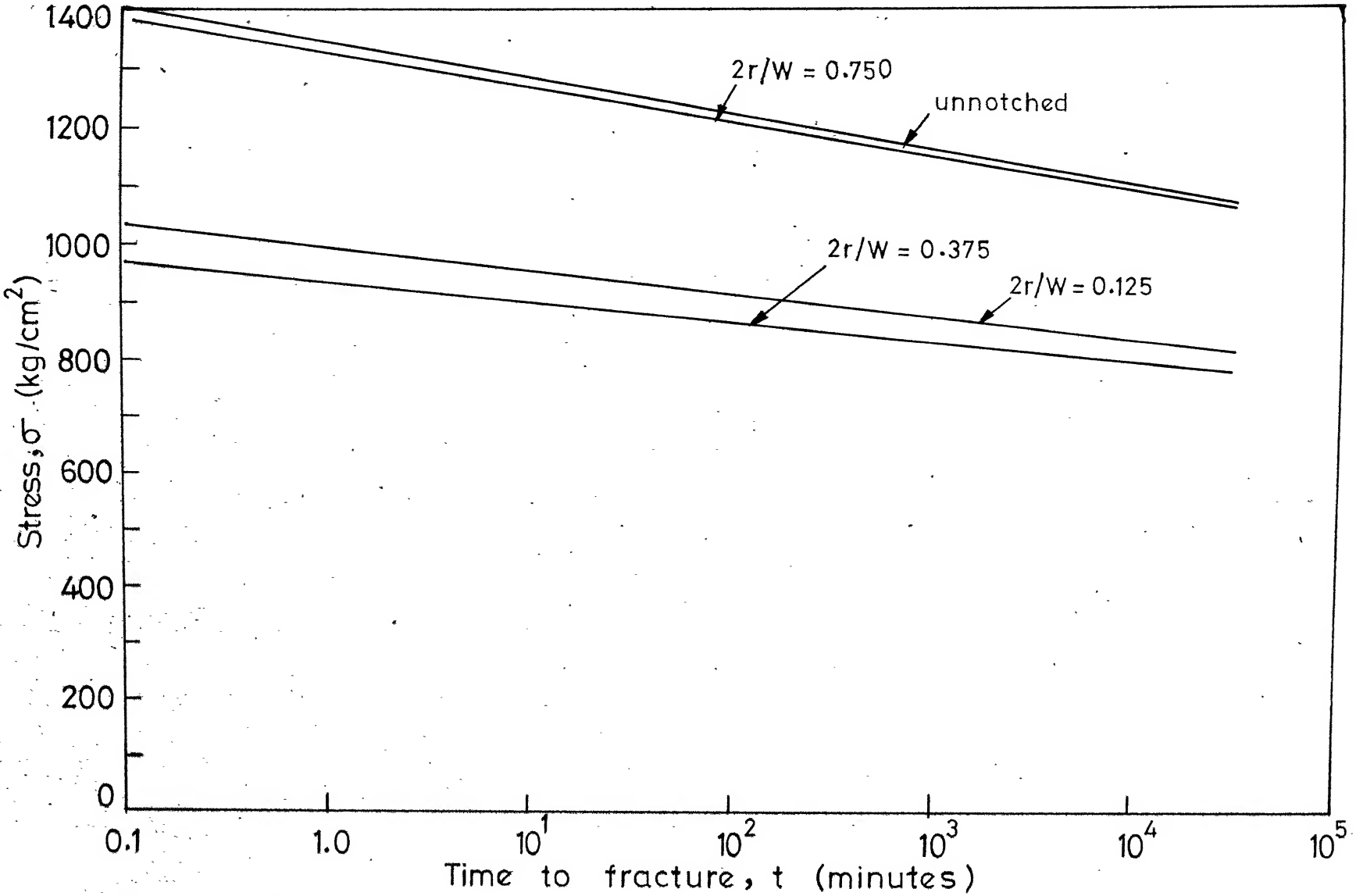

Fig.4.2 Stress vs. time to fracture, for notched and unnotched specimens of 0° composite

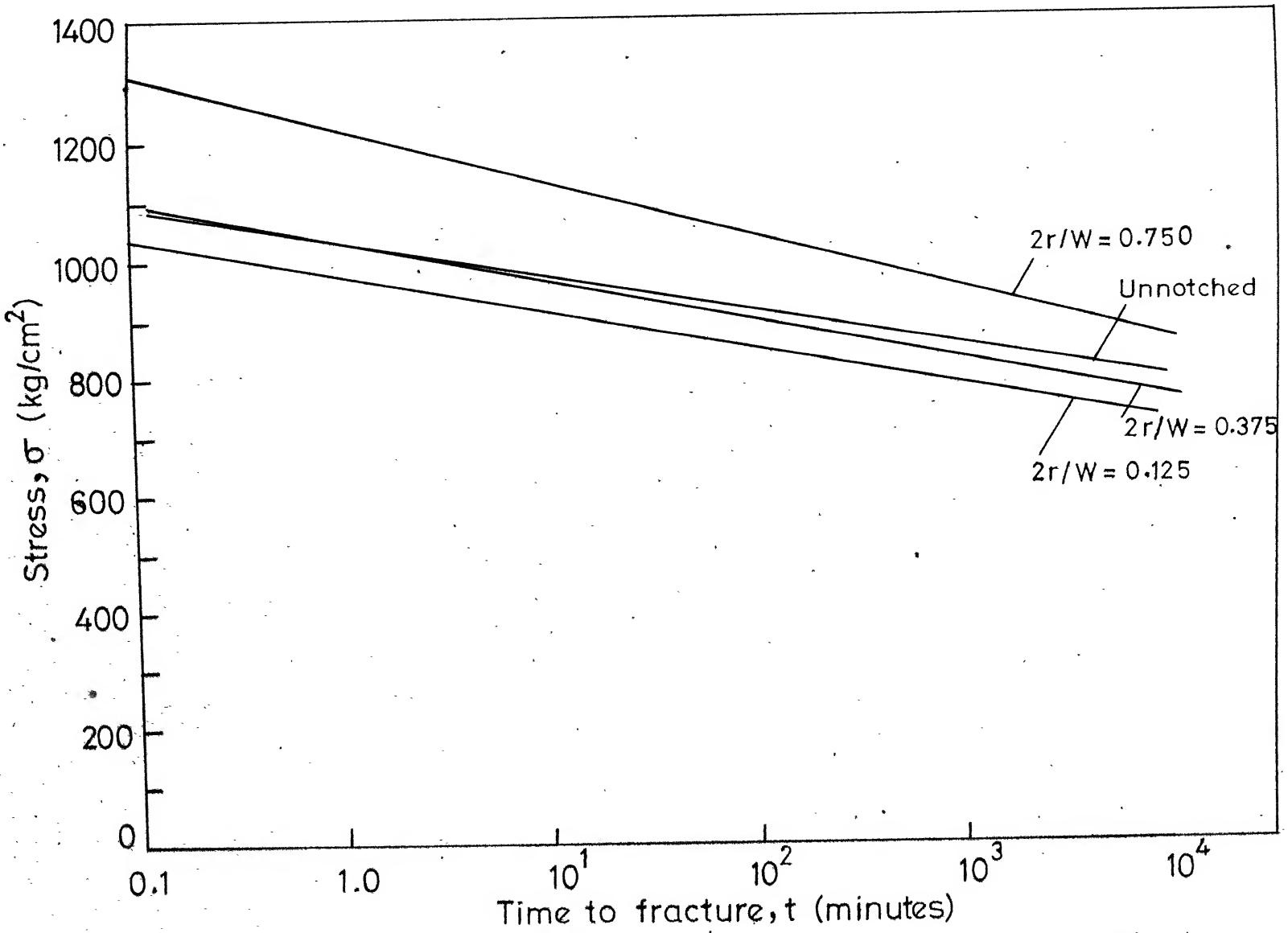

Fig.4.3 Stress vs. time to fracture for notched and unnotched specimens of 45° composite

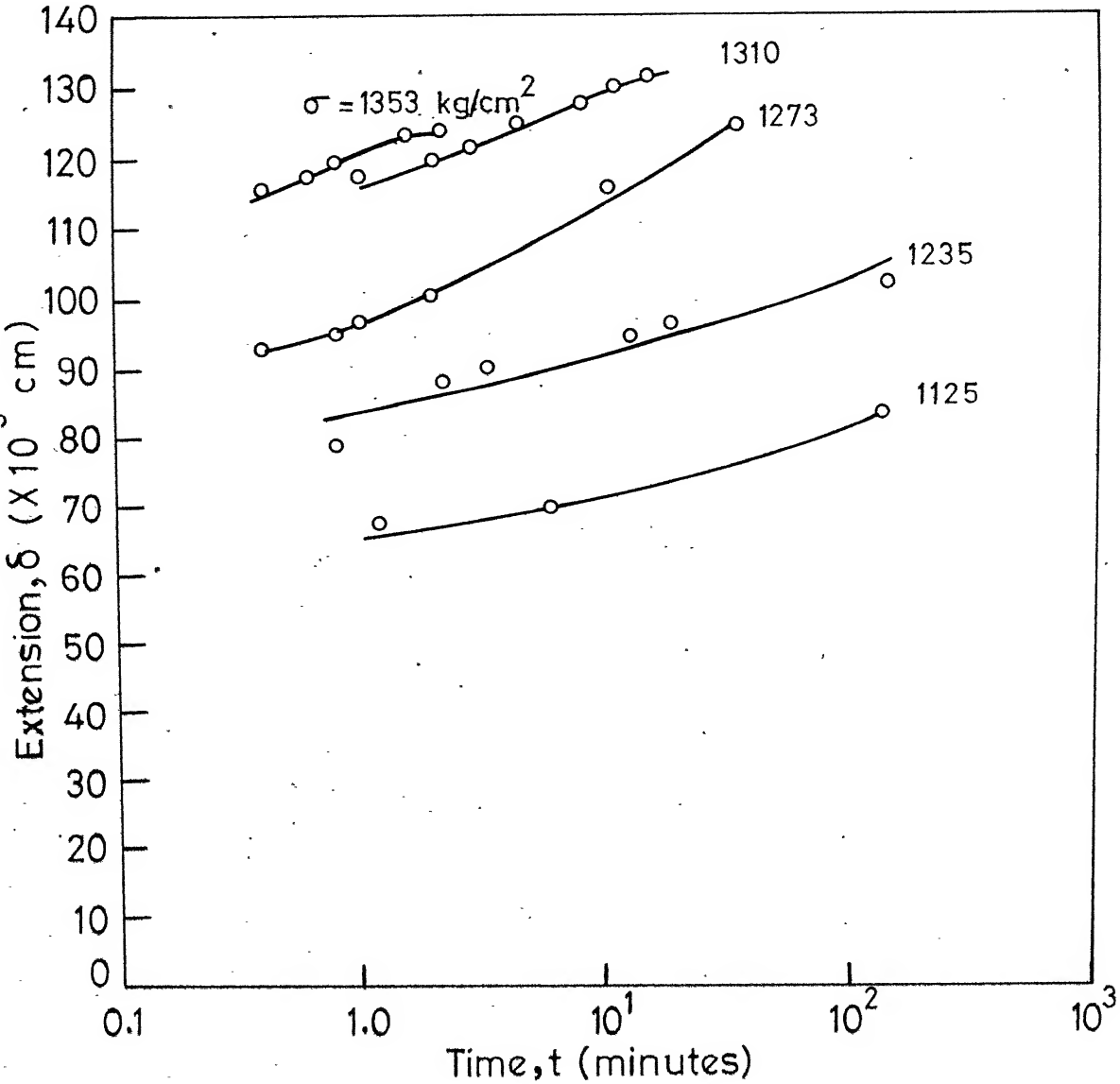

Fig. 4.4 Extension as a function of time for unnotched specimens of 0° composite

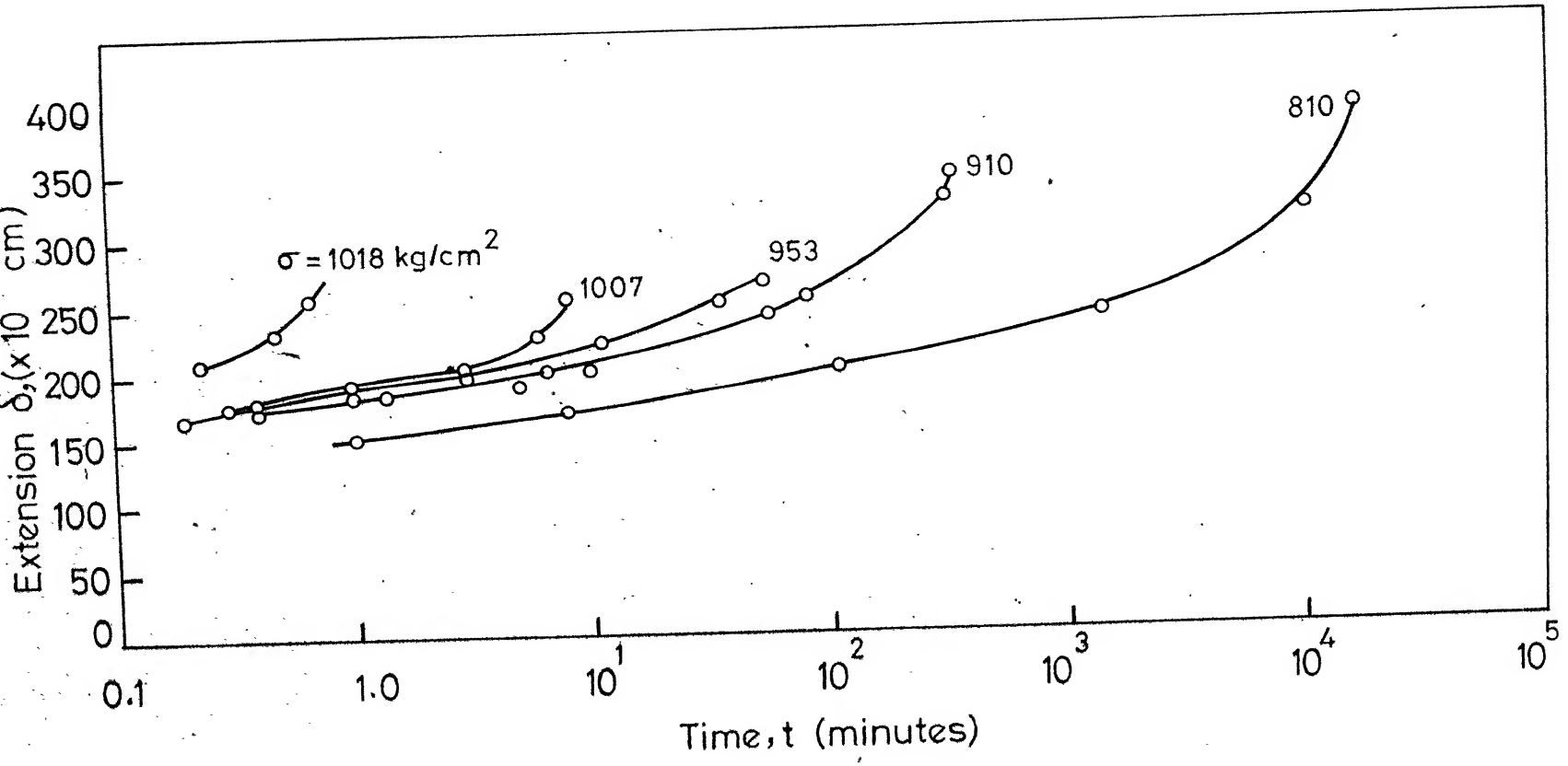

Fig. 4.5 Extension as a Function of time for unnotched specimens of 45° composite

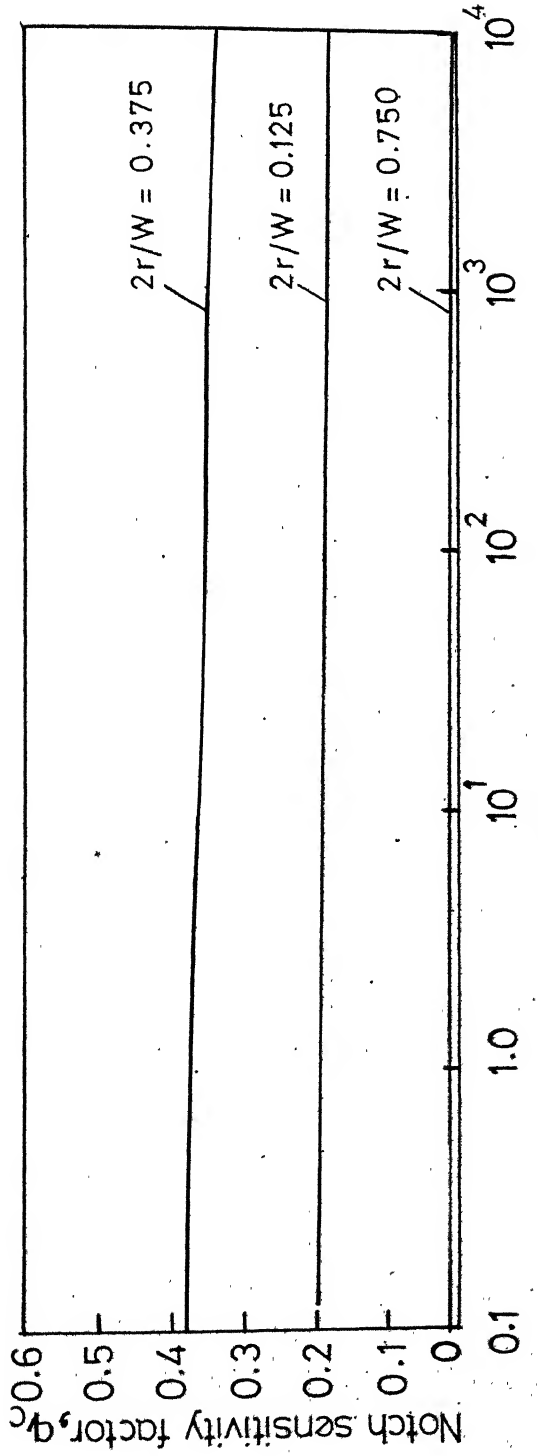

Fig. 4.6 Notch sensitivity factor as a function of time for 0° composite

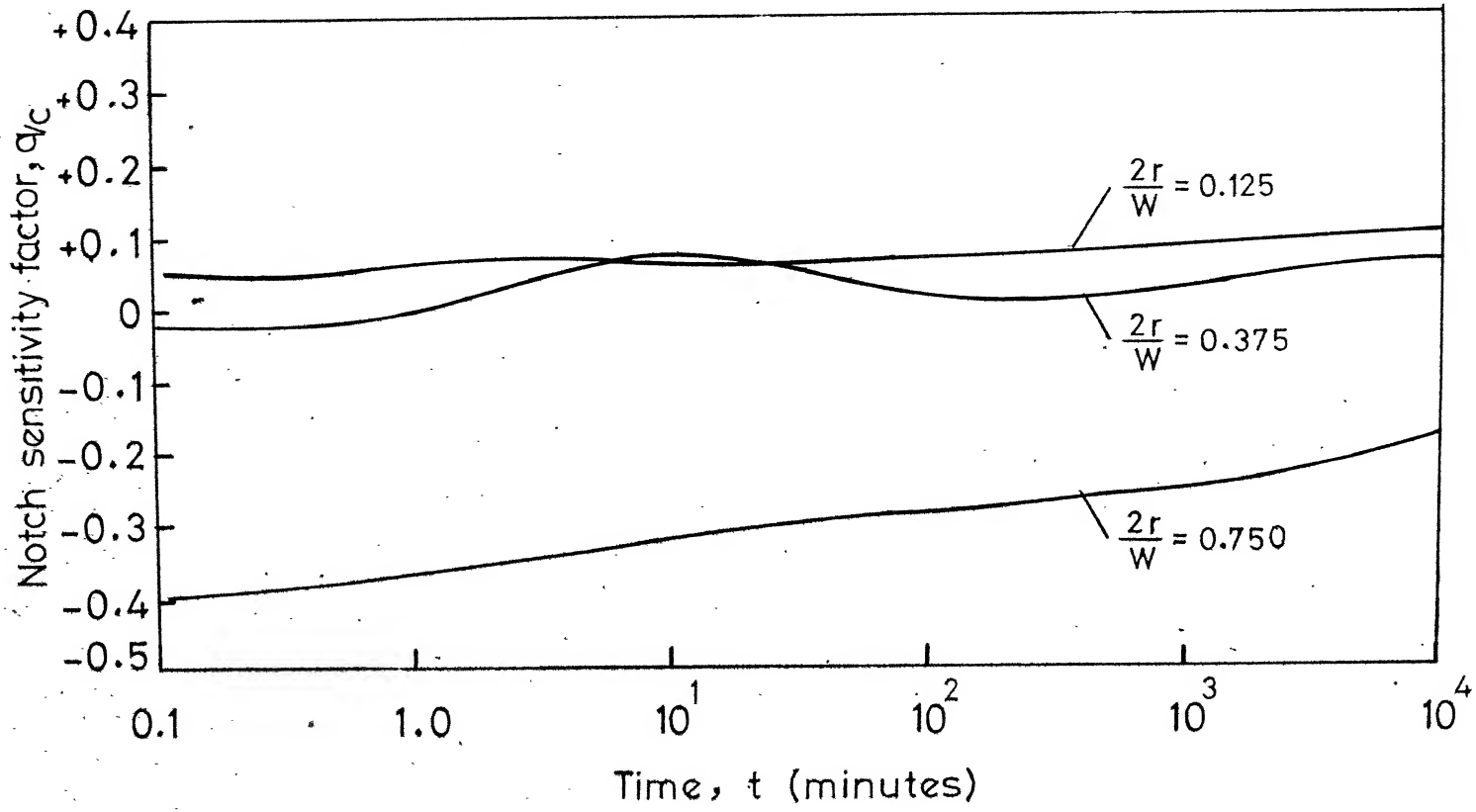

Fig.4.7 Notch sensitivity factor as a function of time for 45° composite

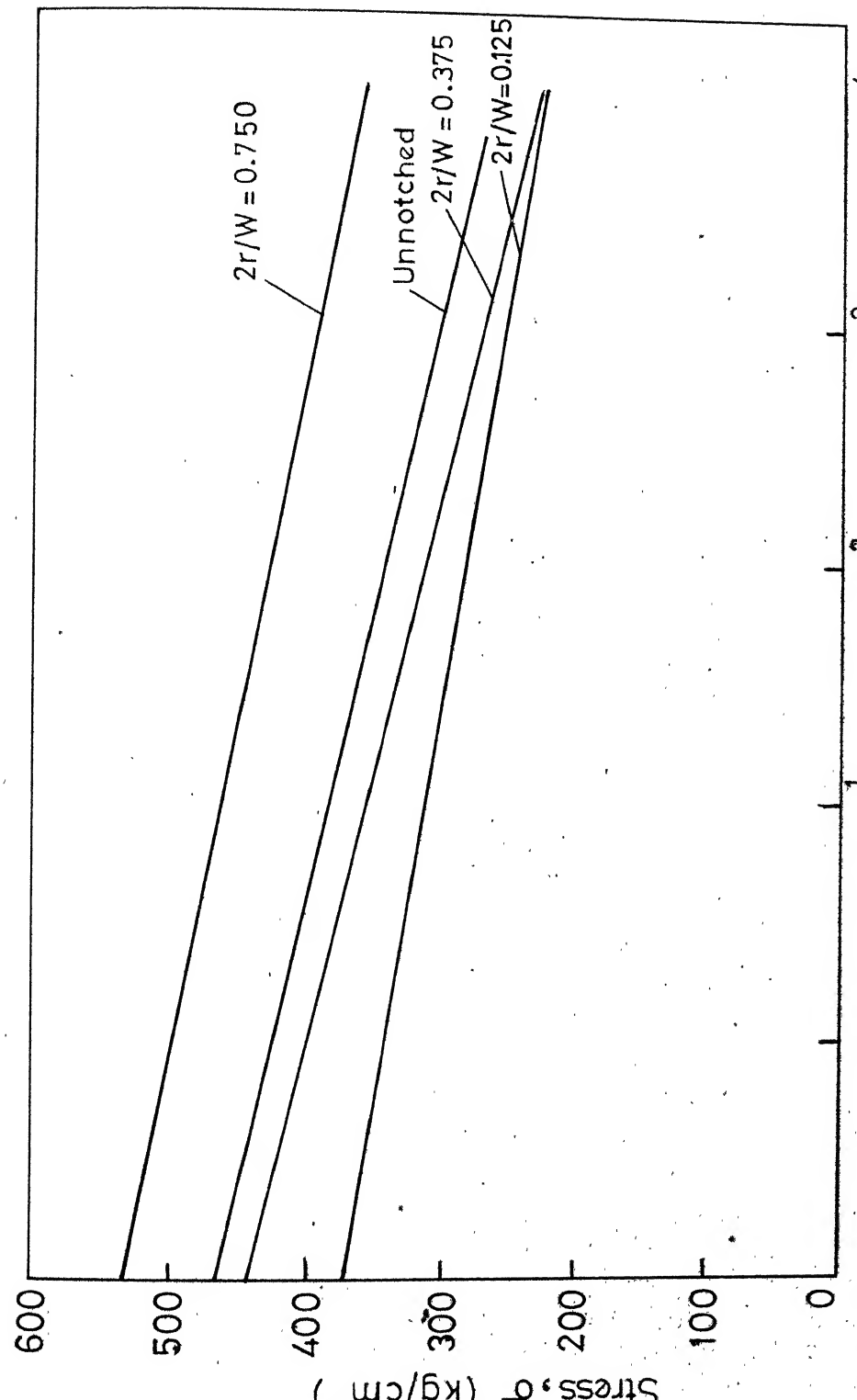

Fig. 4.8 Stress vs. time to fracture, for notched and unnotched specimens of CY-230 epoxy.

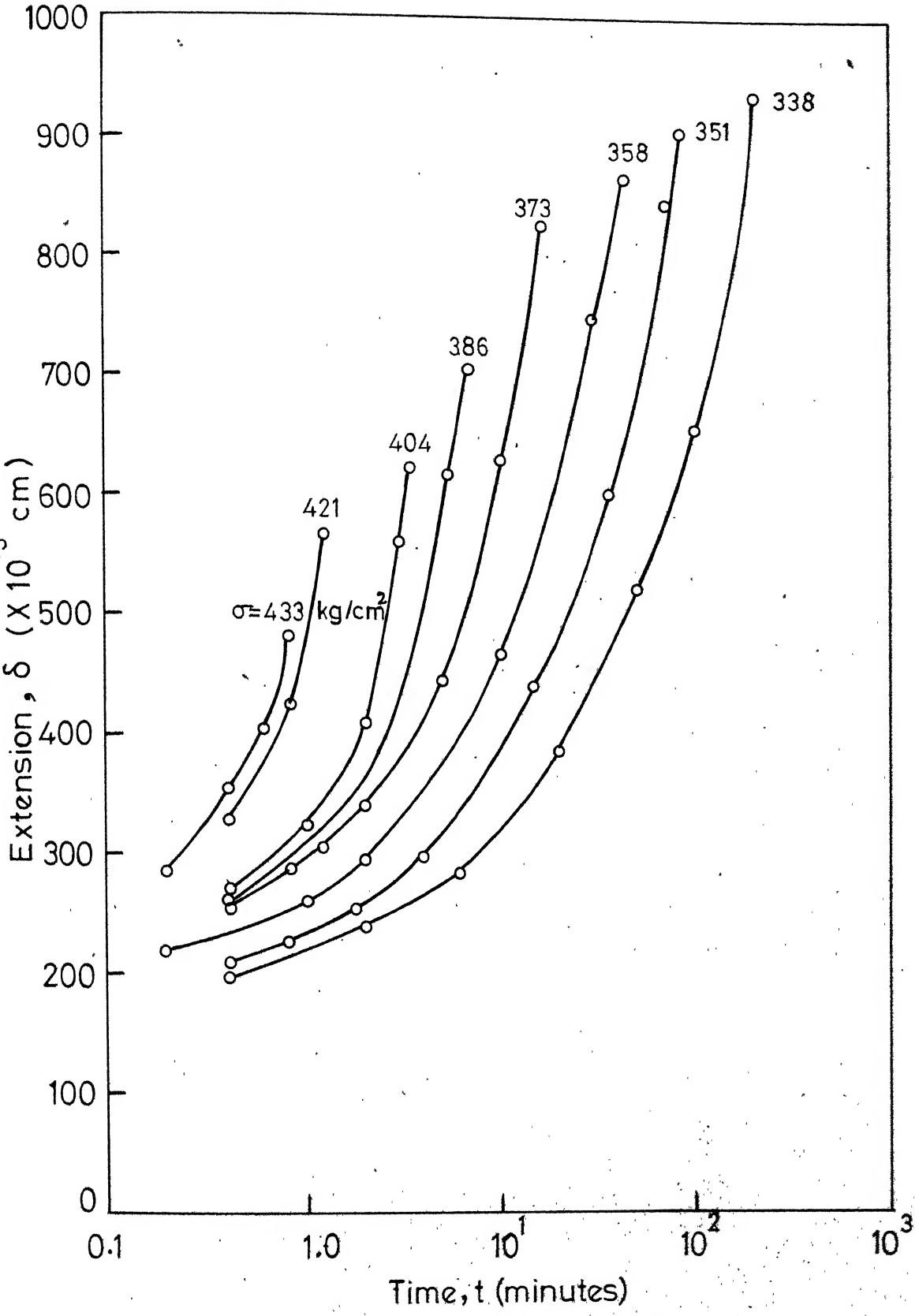

Fig.4.9 Extension as a function of time for unnotched specimens of CY-230 epoxy

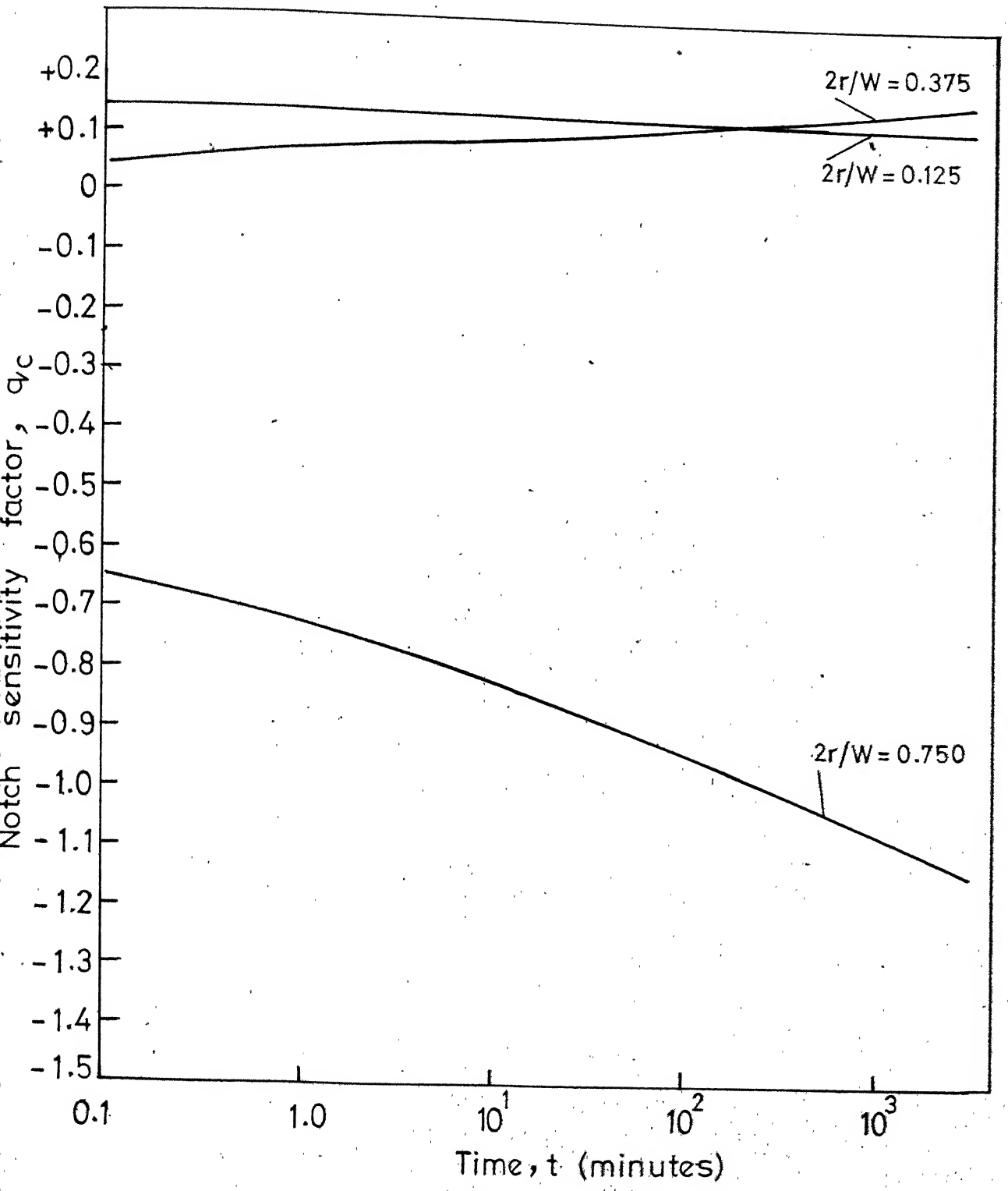

Fig.4.10 Notch sensitivity factor as a function of time for CY-230 epoxy

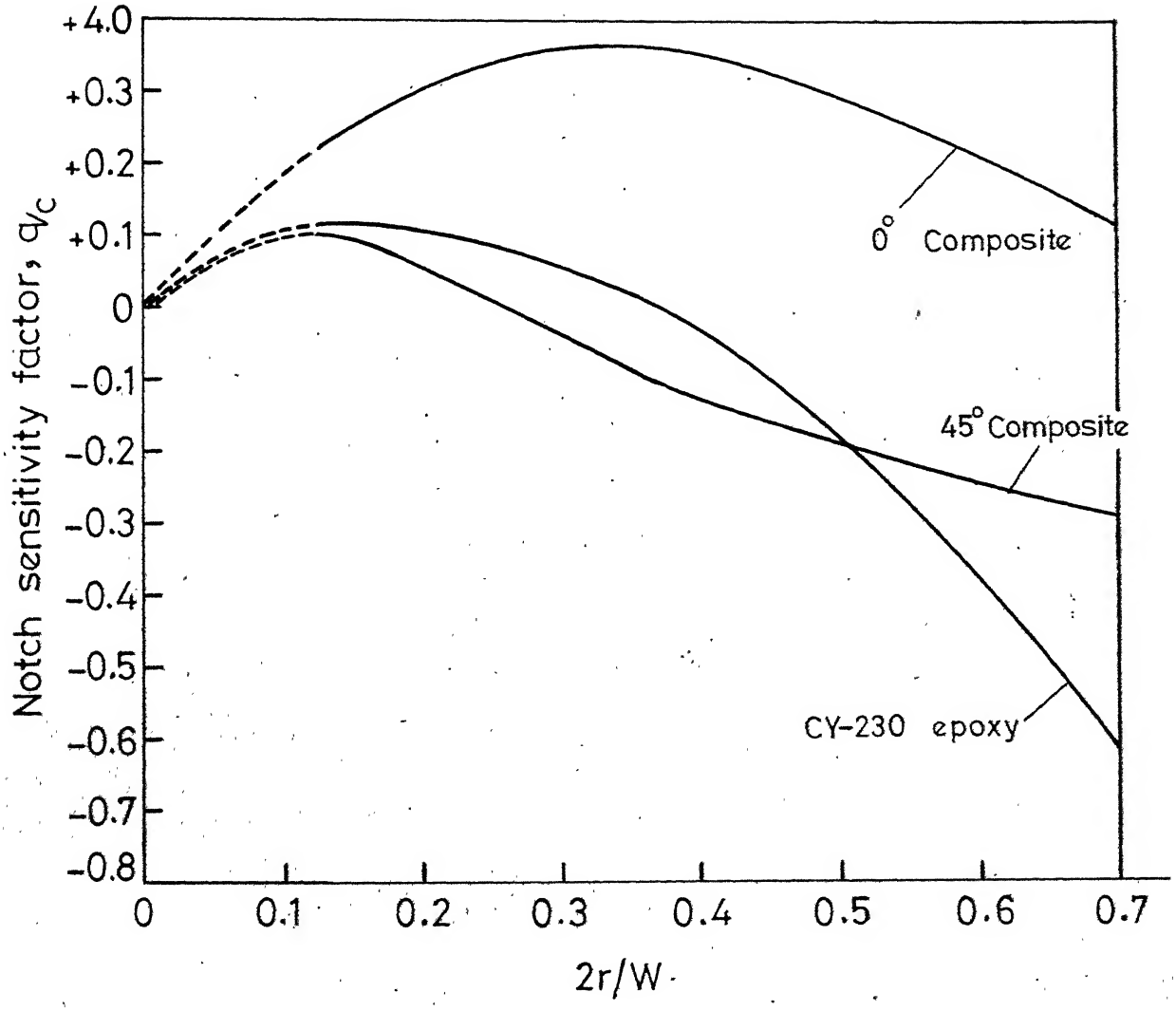

Fig. 4.11 Notch sensitivity factor (based on static test results) as a function of 2r/W for composite and CY - 230 epoxy.

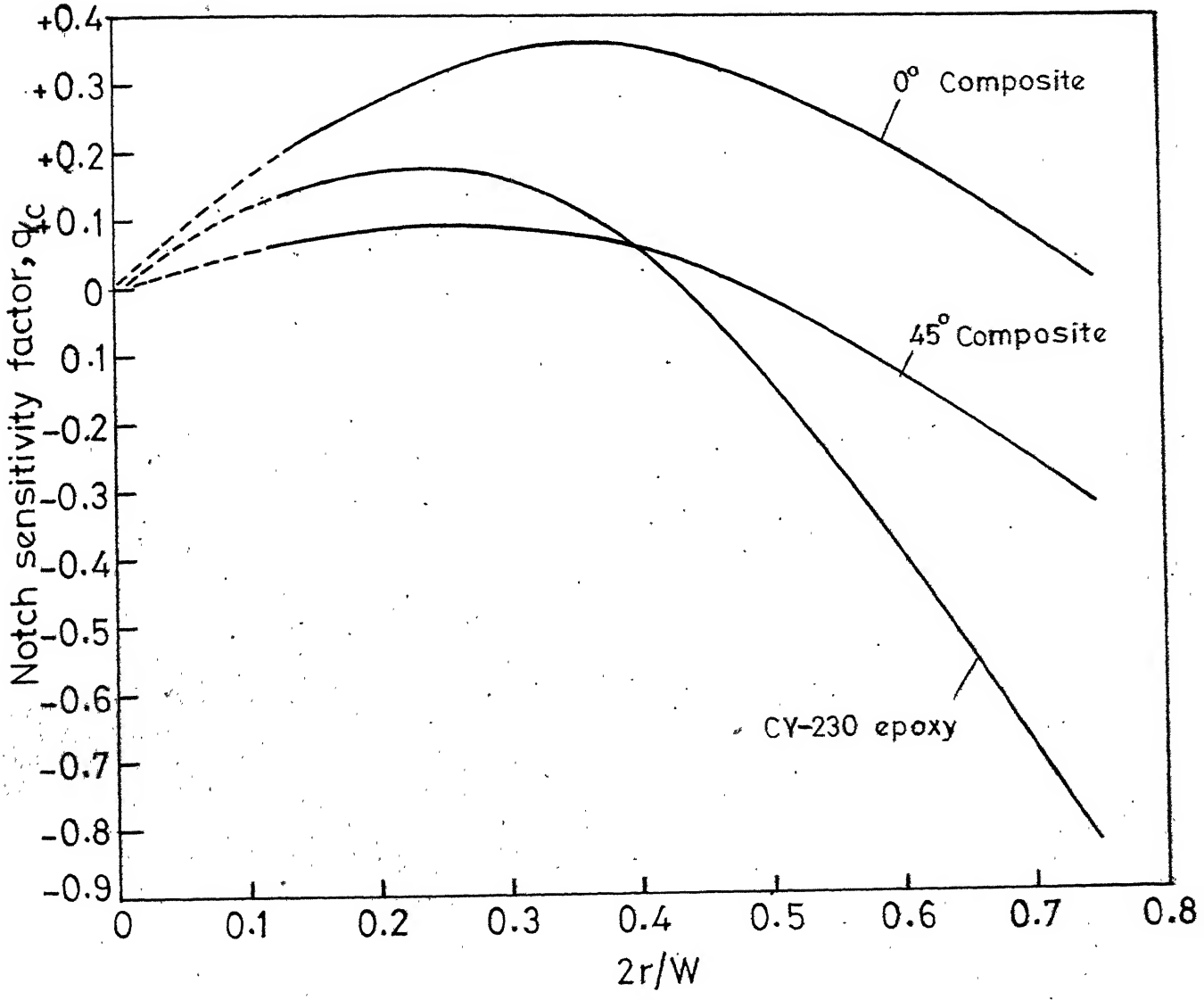

Fig. 4.12 Notch sensitivity factor (based on 10 minutes creep test results) as a function of 2r/W for composite and CY - 230 exopy

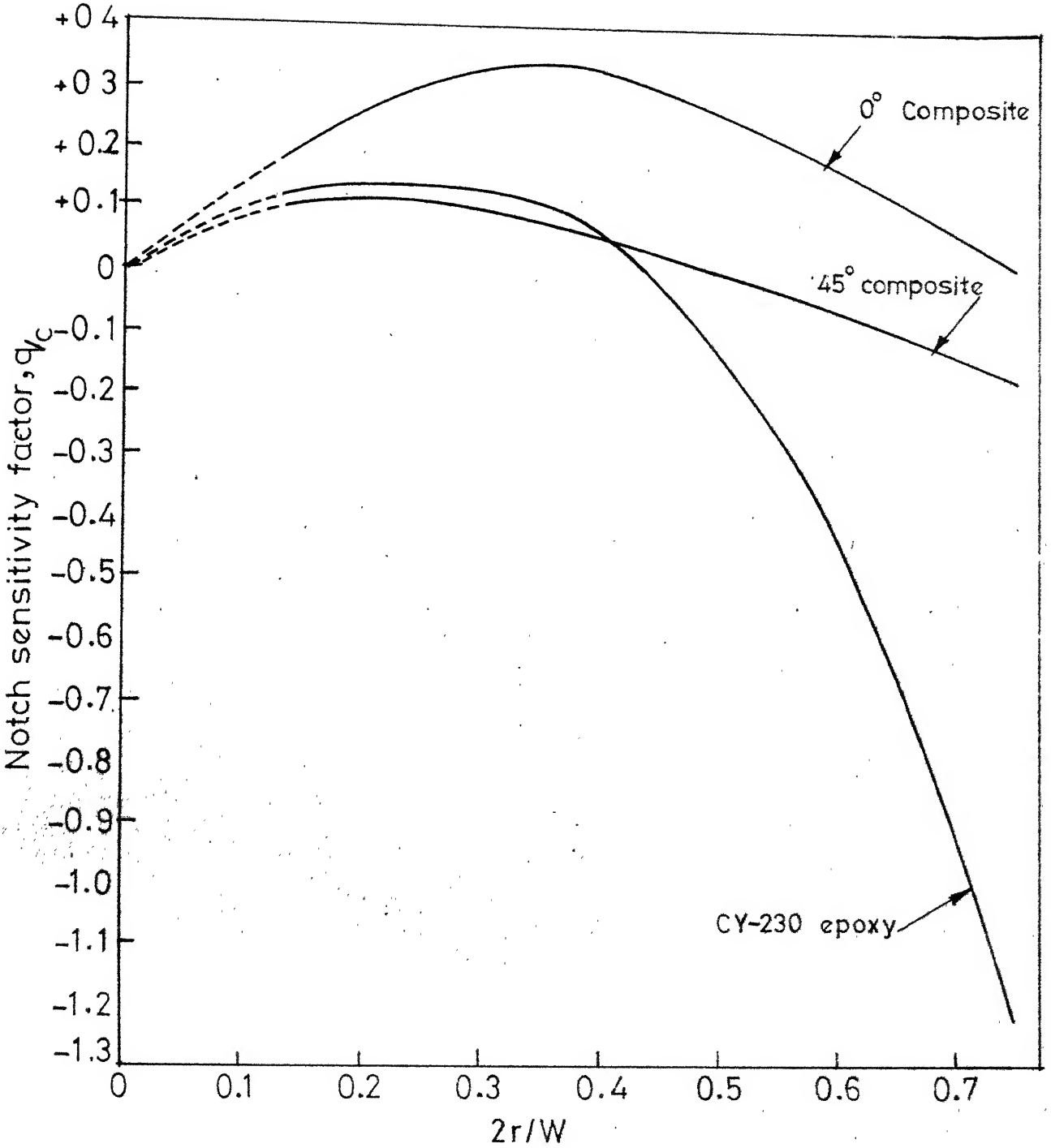

Fig.4.13 Notch sensitivity factor (based on 10^4 minutes creep test results) as a function of 2r/W for composite and CY-230 epoxy

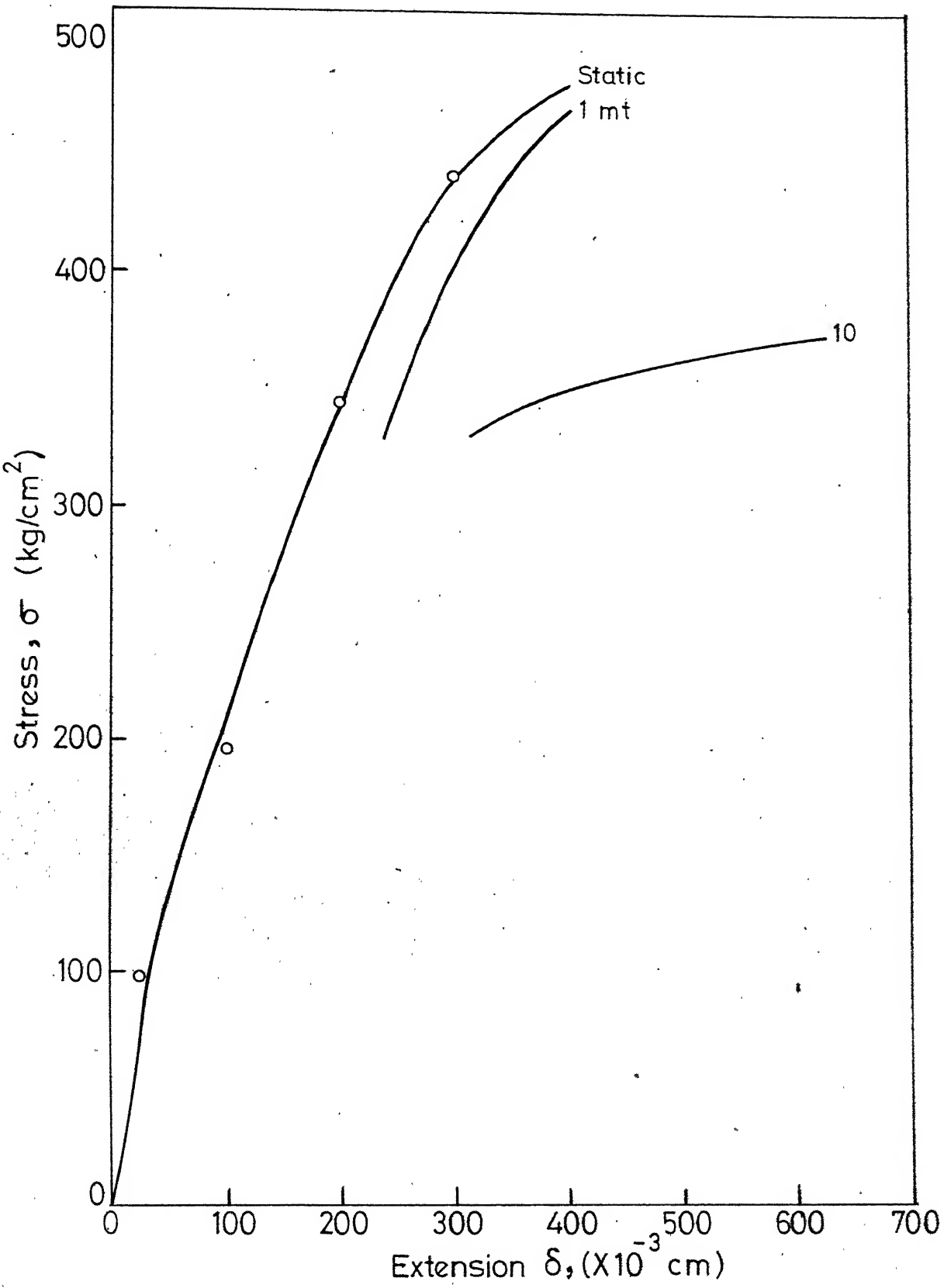

Fig. 4.14 Isochronous stress strain curves for unnotched specimens of CY-230 epoxy

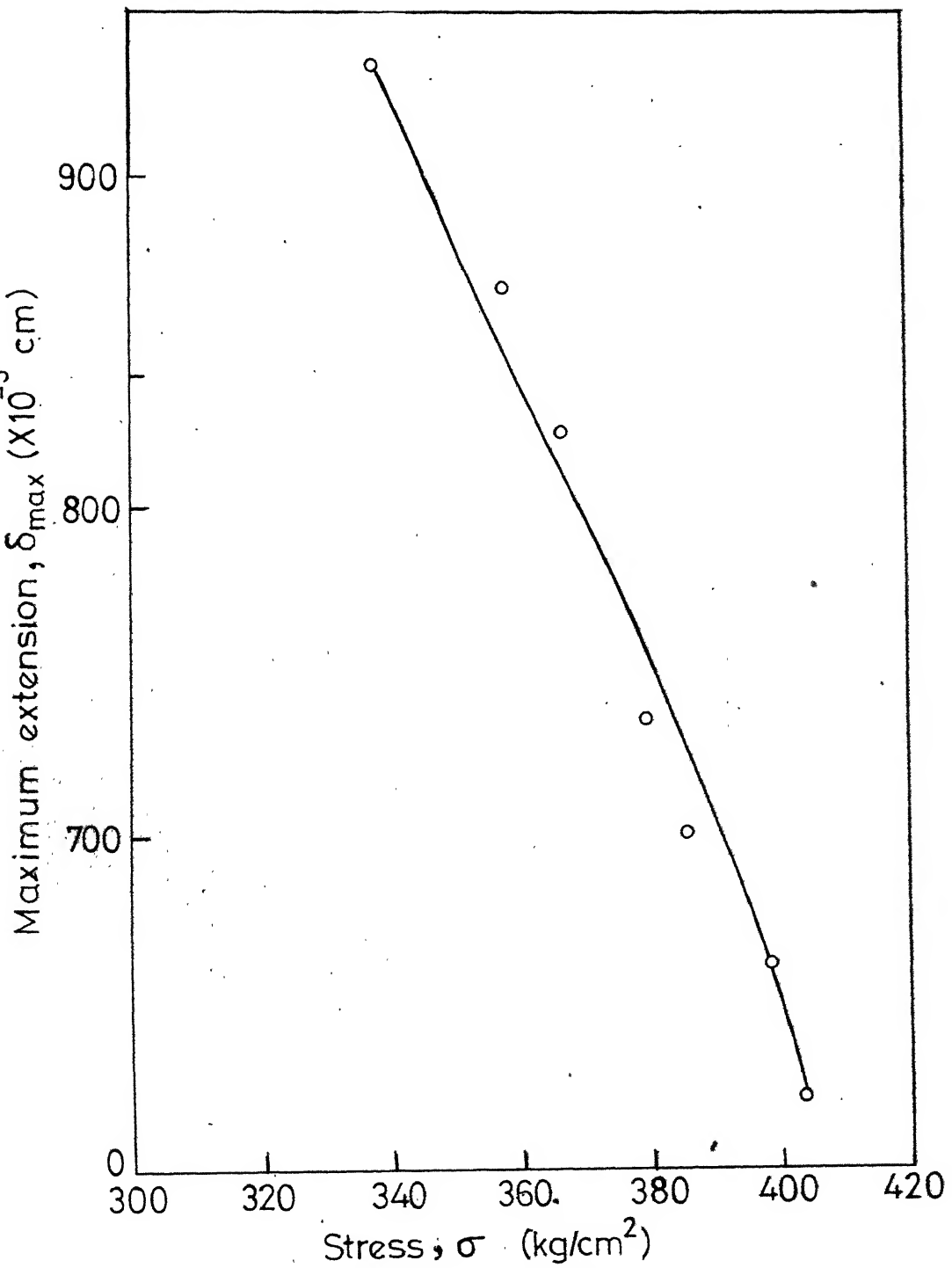

Fig. 4.15 Maximum extension at fracture vs. stress, for unnotched specimens of CY-230 epoxy

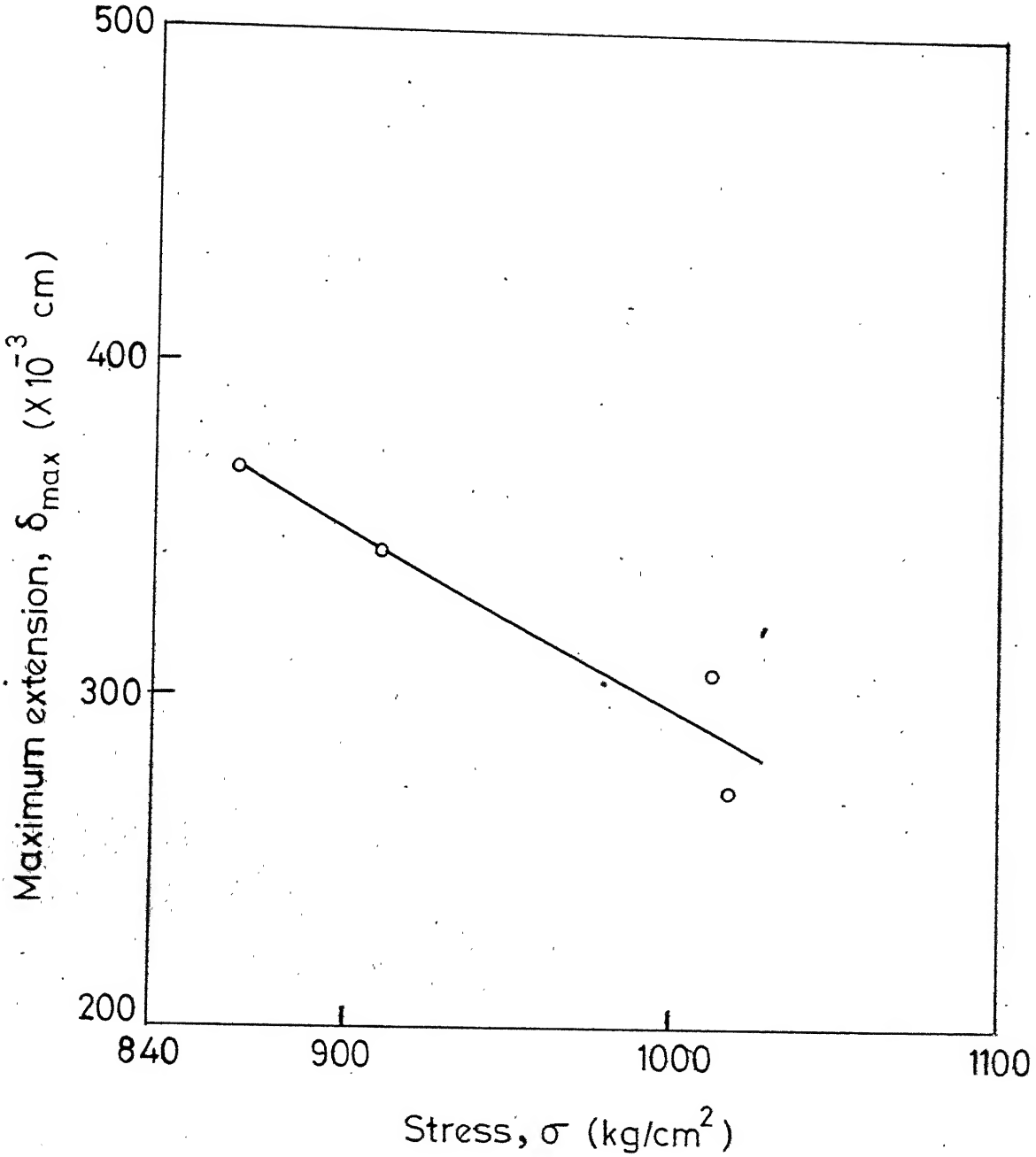

Fig. 4.16 Maximum extension at fracture vs. stress, for unnotched specimens of 45° composite

CHAPTER-V

CONCLUSIONS

A simple but very effective creep testing machine has been designed and fabricated for creep testing of glass fibre reinforced plastics. Although provision has been made in the machine for studying the creep behaviour of GFRP materials at elevated temperatures (upto a maximum of about 300°c), actual testing was done only at room temperature.

Some special features were built into the machine. In view of the high strength of GFRP materials, a large lever ratio of about 35 was provided, so that specimens of standard size (0.12 cm wide and 0.6 cm thick) could be subjected to stresses approaching the static tensile strength. By using a double-lever mechanism, this large lever ratio was achieved in a fairly small space. Another special feature of the creep setup was the Peaucellier cell mechanism to ensure that the specimen was subjected to only an axial load. In view of the fairly large creep extensions that could be expected, an axial loading had to be ensured not only at the time of loading but also at all other times.

In view of the large number of specimens to be tested in any creep investigation, five creep machines were built. Each creep setup was calibrated for the lever ratio and also for corrections due to the elastic deformations of the linkages.

A bidirectionally reinforced commercial composite was tested under creep loading. The fibre orientation angle was intended to be a variable but due to material shortage, only the 0° and 45° orientations were studied. Semicircular side notched tensile strips were tested and the notch parameter $2r/w$ was varied in the case of both orientations. The creep notch sensitivity factor, q_c, was determined by comparing the notched creep rupture strength and the unnotched creep rupture strength and then comparing the creep rupture strength reduction factor with the theoretical stress concentration factor. The 'theoretical stress concentration factors' for the three notch parameters were determined by employing the techniques of photo-orthotropic-elasticity.

The creep notch sensitivity factor, q_c, was found to be positive but small in the case of 0° orientation for all the three notch sizes. For the 45° orientation, a notch strengthening effect was observed in the case of the biggest notch.

The matrix plays a very important role in a composite when the reinforcement direction makes an angle 45° to the load direction. Therefore, it is reasonable to infer that the notch strengthening effect observed for the 45° composite must be due to the matrix. A particular epoxy resin, CY 230, which was found to display a notch strengthening effect in low cycle fatigue, was tested in creep. The polymer exhibited a notch strengthening effect in creep also, especially in the case of the biggest notch.

The consequences of a matrix imparting notch strengthening to the composite, especially in the 45° orientation, are significant. If creep loading of composites and the presence of geometrical discontinuities in composite structures are unavoidable, loading along the weaker directions of the composite (such as the 45° orientation) is also inevitable. The elastic constants, static strength and fatigue strength being less for the 45° orientation compared to the 0° orientation, a notch strengthening effect should be welcome to the designer of composite structures.

Considerable work is necessary to understand the role of stress concentrations on the creep rupture strength of polymers and the role of the matrix in the creep behaviour of the composites before the notch strengthening effect can

be used in the design of composite structures. But the results obtained in this investigation suggest that there may be a relationship between the creep behaviour and the low cycle fatigue behaviour. If such a relationship can be established, then considerable savings in testing time and expenditure can be effected.

REFERENCES

1. Dally, J.W., Carillo, D. and Prabhakaran, R., "Effect of Notches on the Fatigue Behaviour of Continuously Reinforced Composite Materials", Recent Advances in Engineering Science, Vol 6, Edt. A.C. Eringen, Gordon and Breach, Science publishers, Inc., 1968.

2. Prabhakaran, R., "Effect of Notches on Low Cycle Fatigue Failure of Crossply Composites", Proceedings of the International Conference on Composite Material 1975.

3. Nair, E.M.S., "Anisotropy of Notch Sensitivity of Glass Fibre Reinforced Plastics in Low Cycle Fatigue", Thesis submitted for degree of M. Tech., Department of Mechanical Engineering, I.I.T., Kanpur, July 1976.

4. Dally, J.W. and Alfirevich I., "Stress Concentration Factors in Anisotropic Materials", Army Symp. Solid Mech., Monograph Series, AMMRC-MS-68-09, pp 235-253, (1968).

5. Dally, J.W. and Prabhakaran, R., "Photo-orthotropic Elasticity", Experimental Mechanics, Vol. 11 (1971), p. 346.

6. Pih, R. and Knight, C.E., "Photoelastic Analysis of Anisotropic Fibre Reinforced Composites", Journal of Composite Materials Vol. 3 (1969), p. 94.

7. Sampson, R.C., "A Stress Optic Law for Photoelastic Analysis of Orthotropic Composites", Experimental Mechanics, Vol. 10 (1970), p. 210.

8. Peterson, R.E., "Stress Concentration Factors", Pub. John Wiley and Sons, Inc., 1974.

9. Schapery, R.A., "Viscoelastic Behaviour and Analysis of Composite Materials", Tex A & M Univ, College Station, Composite Mater. Vol. 2, 1974, p. 85-168.

10. Weidmann, G.W. and Ogorkiewicz, R.M., "Tensile Creep of a Unidirectional Glass Fibre-Epoxy Laminate", Composite, Volume 5, Number 3, May 1974, pp. 117-21.